

A consistent regional dataset of dissolved oxygen in the Western Mediterranean Sea (2004-2023): CTD-O₂WMED

Malek Belgacem¹, Katrin Schroeder¹, Marta Álvarez², Siv K. Lauvset³, Jacopo Chiggiato¹, Mireno Borghini⁴, Carolina Cantoni⁵, Tiziana Ciuffardi⁶, Stefania Sparnocchia⁵

¹ CNR-ISMAR, Arsenale Tesa 104, Castello 2737/F, 30122 Venice, Italy

² Instituto Español de Oceanografía, IEO-CSIC, A Coruña, Spain

³ NORCE Norwegian Research Centre, Bjerknes Centre for Climate Research, Bergen, Norway

⁴ CNR-ISMAR, Via Santa Teresa, Pozzuolo di Lerici, 19032 La Spezia, Italy

⁵ CNR-ISMAR, Area Science Park, Basovizza, 34149 Trieste, Italy

⁶ Department of Sustainability, St Teresa Marine Environment Research Centre, ENEA, Pozzuolo di Lerici, 19032 La Spezia, Italy

Correspondence to: Malek Belgacem (malek.belgacem@ve.ismar.cnr.it)

Abstract.

The Mediterranean Sea is experiencing rapid environmental changes, underscoring the urgent need for high-quality, long-term datasets to quantify trends and assess impacts on biogeochemical cycles.

Over the past few years much work has been done to improve and ensure data quality in the Western Mediterranean Sea (WMED), but reliable dissolved oxygen (O₂) data remains scarce. This is a critical gap, as oxygen is a key indicator of marine ecosystem health and plays a central role in carbon and nutrient cycling. To address this gap, we compiled and rigorously quality-controlled a new regional-scale WMED dataset of O₂ data from sensors mounted on Conductivity Temperature and Depth (CTD) probes: CTD-O₂WMED. This product includes over 1000 previously unpublished high-resolution vertical profiles of CTD-O₂ measurements mostly collected within Italian cruises between 2004 and 2023. The quality control process involved sensor post-calibration against discrete Winkler measurements, primary screening, and a secondary check based on crossover analysis with reference datasets. Combined this ensures the consistency of the final corrected CTD-O₂WMED across both space and time. CTD-O₂WMED provides a robust observational foundation for assessing trends of dissolved oxygen variability, mainly associated with climate change, anomalies related to deoxygenation processes, and contributes to advancing our understanding of ventilation processes in the WMED. It also serves as a benchmark for calibrating biogeochemical Argo floats and for validating regional biogeochemical models.

Data coverage

Coverage: 44° N–35° S, 6° W–14° E

Location name: western Mediterranean Sea

Date/time start: October 2004

Date/time end: April 2023

Commented [SL1]: Since one reviewer commented that mentioning a previous paper so prominently in the abstract is a bit strange (and I agree that references should be avoided in the abstract) I suggest we revise this to something along these lines:

Over the past few years much work has been done to improve and ensure data quality in the Western Med Sea, but reliable dissolved oxygen data remain scarce

1 Introduction

Dissolved oxygen (O₂) in the ocean is primarily produced through photosynthesis by phytoplankton in the surface layer, especially in regions of high primary productivity. The subsequent export and remineralization of organic matter from the surface lead to oxygen consumption at depth, potentially giving rise to oxygen minimum zones (OMZs) or oxygen minimum layers (OMLs), where biological respiration exceeds oxygen supply. While OMZs are characteristic of certain oceanic regions, the Mediterranean Sea is generally well-oxygenated and does not develop OMZs, but rather OMLs (Álvarez et al. BOOK). Nonetheless, localized low-oxygen events may become more frequent and intense in response to ongoing climate change and human activities driving eutrophication events (Grégoire et al. 2023).

Ocean warming and increased stratification reduce oxygen solubility and inhibit vertical mixing, respectively, thereby limiting the downward transport of oxygen-rich surface waters. These processes contribute to the expansion and intensification of low-oxygen zones, with important consequences for biogeochemical cycling, ecosystem functioning, and carbon export (Keeling et al., 2009). In the deep ocean, enhanced remineralization and reduced ventilation can further exacerbate oxygen loss. Under low-oxygen conditions, denitrification may also occur, altering the nitrogen-to-phosphorus (N:P) ratio and influencing both nutrient cycling and primary productivity.

Increased CO₂ concentrations and stratification can also reshape biological communities, potentially lowering ecosystem resilience. These biogeochemical shifts affect the distribution of oxygen and other biogeochemical variables, particularly in semi-enclosed basins like the Mediterranean Sea. In recent decades, the region has undergone significant environmental changes, including recurrent marine heatwaves (Marullo et al., 2023; Martinez et al., 2023; Pastor and Khodayar et al., 2023), which influence oxygen distribution (Reale et al., 2022; Alvarez et al., 2023). The Mediterranean's semi-enclosed configuration, complex thermohaline circulation, and pronounced regional differences make it especially sensitive to climate variability (Powley et al., 2016; Testor et al., 2017; Margirier et al., 2020).

Two major events have notably impacted the thermohaline structure of the Mediterranean Sea. In the Eastern Mediterranean (EMED), the Eastern Mediterranean Transient (EMT) of the mid-1990s shifted ~~to be the source of~~ deep-water formation source from the colder, less saline Adriatic Deep Water to warmer, saltier Aegean/Cretan Water. This new deep-water mass ventilated the Levantine basin and the Ionian Sea around 1999 and reached the Sicily Channel by 2001 (Schroeder et al., 2006). When the Aegean contribution weakened, the Adriatic source regained dominance between 2000 and 2010. However, in subsequent years, it failed to reach the deepest Ionian layers, ventilating instead the 2000-3000 m depth range. In the Western Mediterranean Sea (WMED), deep convection in the Gulf of Lion has traditionally ensured ventilation of the Western Mediterranean Deep Water (WMDW). A peak in deep water renewal occurred during the Western Mediterranean Transition (WMT) in year 2005 (Schroeder et al., 2016). Since then, a decline in both frequency and intensity of deep convection has been observed (Fourrier et al., 2020; Li and Tanhua, 2020), leading to reduced deep layer ventilation and an intensification of the oxygen minimum at intermediate depths, with implications for the uptake of atmospheric oxygen (Ulses et al., 2021). Long-term observational programs such as the MEDAR/MEDATLAS (Fichaut et al., 2003), Med-SHIP (Schroeder et al., 2015), RADMED (Lopez-Jurado et al., 2015), and the MOOSE network (Coppola et al., 2018) have provided crucial insights into these changes. Recently, machine learning techniques

Formatted: Font: +Headings CS (Times New Roman), 10 pt, Bold, Font color: Text 1, Complex Script Font: 10 pt, Bold

Formatted: Outline numbered + Level: 1 + Numbering Style: 1, 2, 3, ... + Start at: 1 + Alignment: Left + Aligned at: 0 cm + Indent at: 0,63 cm

Commented [SL2]: This sentence needs a bit more clarification. Is the EMT the location of deep water formation? And then the source water changed in the 1990s? Please revise to make it easier to understand (and remove one of the "source")

Commented [SL3]: This topically belongs with the paragraph above

Commented [SL4]: This is still topically the same paragraph as the two above

77 have been employed to reconstruct oxygen fields at higher spatial and temporal resolution using satellite and
78 auxiliary data sources (Liu et al., 2025). Nevertheless, substantial uncertainties in the quantification and long-term
79 impacts of O₂ changes on Mediterranean Sea marine ecosystems still remain (Coppola et al., 2018; Alvarez et al.
80 2014).

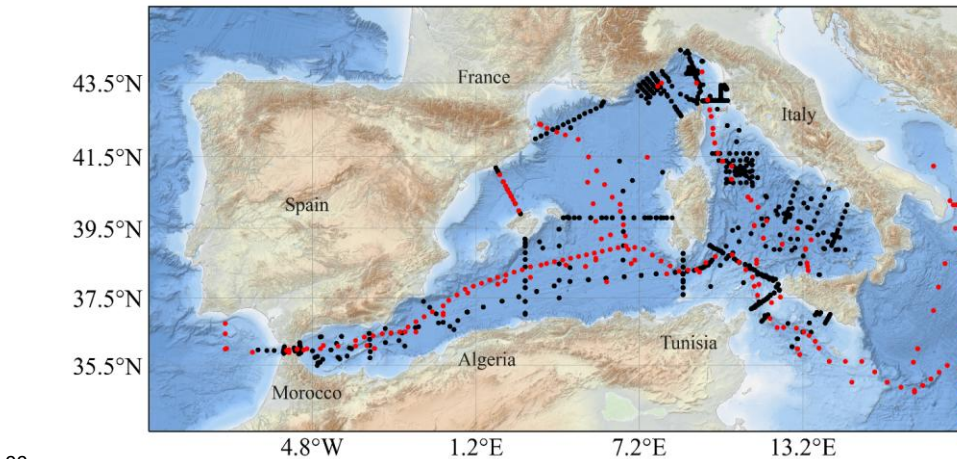
81 To improve our understanding of regional dissolved oxygen dynamics and the impact of climate changes on
82 biogeochemical trends, this study presents a quality-controlled compilation of CTD oxygen profiles collected by
83 the Italian National Research Council (CNR) between 2004 and 2023 in the WMED. The dataset provides reliable
84 CTD-based oxygen measurements that support assessments of water mass ventilation and long-term variability.
85 This paper documents the dataset and outlines the quality control procedures, including calibration assessment
86 against discrete Winkler measurements, first quality control flagging- and secondary quality corrections, to ensure
87 the consistency of the CTD oxygen data product released, CTD-O₂WMED.

88 2 Dissolved oxygen data collection

89 2.1 The CNR data collection

90 The CTD-Oxygen in the WMED (CTD-O₂WMED) dataset comprises 1382 dissolved oxygen profiles collected
91 with CTD probes across 25 CNR research cruises (Table 1). Figure 1 shows the spatial distribution of these
92 profiles, illustrating broad coverage throughout the northern WMED and along key hydrographic transects. The
93 majority of measurements are concentrated in the eastern portion of the WMED, including the Ligurian and
94 Tyrrhenian Seas, and the Tunisia-Sicily-Sardinia region.

95 Spanning the period from 2004 to 2023, the dataset provides robust temporal coverage, particularly from 2004 to
96 2015 (see Figure 2a). Notably, the years 2005, 2006, 2010, and 2012 comprise the highest number of CTD stations,
97 coinciding with monthly surveys (Figure 2). While the temporal distribution remains consistent between 2004 and
98 2015 (except for 2014), the number of sampled stations decreases significantly after 2016.



99
100 **Figure 1.** Spatial distribution of cruise stations with CTD oxygen data (black dots) in the CTD-O₂WMED dataset.
101 The red markers indicate stations (discrete Winkler measurements) from the reference dataset.

Formatted: Font: +Headings CS (Times New Roman),
10 pt, Bold, Font color: Text 1, Complex Script Font: 10
pt, Bold

Formatted: Space After: 12 pt, Line spacing: Multiple
1,08 li, Outline numbered + Level: 1 + Numbering Style:
1, 2, 3, ... + Start at: 1 + Alignment: Left + Aligned at: 0
cm + Indent at: 0,63 cm

Formatted: Heading 3, Space After: 12 pt, Line
spacing: single, Outline numbered + Level: 2 +
Numbering Style: 1, 2, 3, ... + Start at: 1 + Alignment:
Left + Aligned at: 0,63 cm + Indent at: 1,4 cm

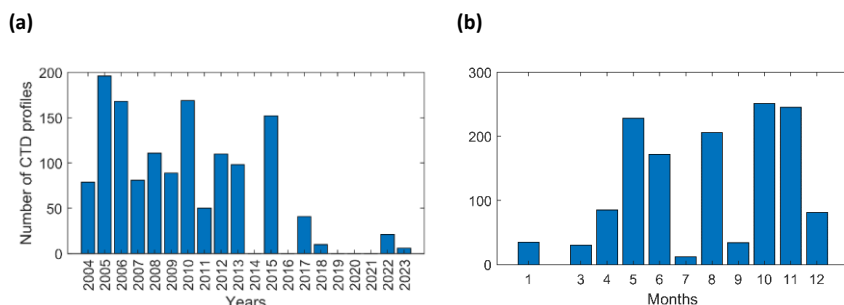


Figure 2. Temporal information about CTD-O₂WMED profiles: (a) annual and (b) monthly distributions.

2.2 Assessment of CTD-O₂ post-calibration

CTD-O₂, which stands for sensor based dissolved oxygen, was measured using Sea-Bird SBE43 sensors mounted on the CTD rosette frame. For each cruise, ~~all variable were checked and dissolved oxygen dataset was first converted to standard units to ensure uniformity. The Gibbs Sea Water (GSW) toolbox (https://www.teos-10.org/pubs/gsw/html/gsw_contents.html) was used to compute conservative temperature (CT), absolute salinity (SA), and potential density.~~ Dissolved oxygen was converted from milliliters per liter (ml L⁻¹) to micromoles per kilogram (μmol/kg) using potential density and the conversion factor 44.66 μmol O₂ L⁻¹, ensuring consistency across datasets. In addition, discrete samples collected at various depths from Niskin bottles were analyzed via Winkler titration onboard. This dataset focuses exclusively on CTD sensor data, so the discrete data are not included in the final product.

~~The Gibbs Sea Water (GSW) toolbox (https://www.teos-10.org/pubs/gsw/html/gsw_contents.html) was used to compute conservative temperature (CT), absolute salinity (SA), and potential density to provide an accurate representation of seawater properties during the 1st quality check process.~~

In the second step the CTD-O₂ data from cruises listed in Table 1 were post-calibrated using Winkler discrete data, following standard protocols (Grasshoff et al. 1983; Langdon, 2010) and accounting for sensor drift and hysteresis in line with the procedures by Janzen et al. (2007) and Uchida et al. (2010). We followed the Sea-Bird Electronics Application Note 64-2 (*SBE 43 DO Sensor calibration and data correction*, www.seabird.com). Residuals between the Winkler (O₂ bottle) and sensor CTD (O₂ sensor) measurements, matched based on pressure, were evaluated after post-calibration, following Uchida et al. (2010) (Figure 3). When more than one SBE43 sensor was deployed during a cruise, the sensor with the lowest residuals relative to Winkler samples was used in the further assessment.

Figure 3a shows the residuals (O₂ bottle – O₂ sensor) plotted against pressure, with cruises color-coded by start date. Differences of up to ±10 μmol/kg are observed especially in the upper 800 dbars. Figure 3b summarizes residual distributions for each cruise using whisker plots, where it is easy to identify cruises with high variability (standard deviation of the mean residual > 7 μmol/kg): 48UR20041006, 48UR20050412, 48UR20080905, and 48QL20171023. For cruise 48UR20080905, only five Winkler samples were available, which limited the post-

Formatted: Font: +Headings CS (Times New Roman), 10 pt, Bold, Font color: Text 1, Complex Script Font: 10 pt, Bold

Formatted: Heading 3, Space After: 12 pt, Line spacing: single, Outline numbered + Level: 2 + Numbering Style: 1, 2, 3, ... + Start at: 1 + Alignment: Left + Aligned at: 0,63 cm + Indent at: 1,4 cm

Commented [SL5]: I don't understand why this is included. What is it explaining?

Field Code Changed

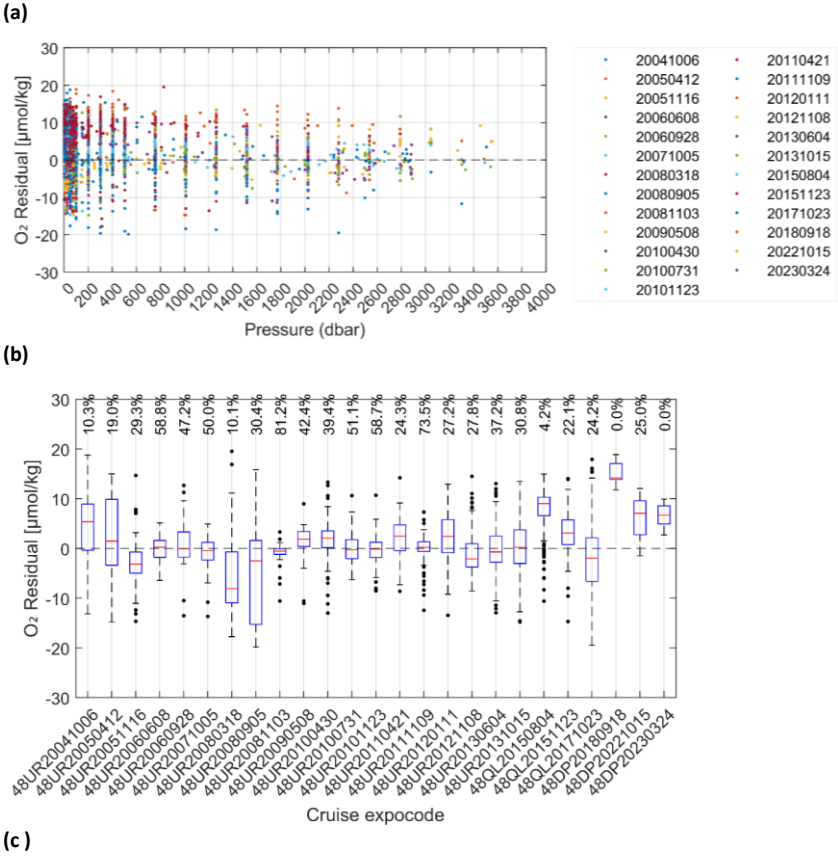
Commented [MB6]: Line 260: Why use absolute salinity? The convention is to use PSU for data and data products, and do the conversion to absolute salinity in a second step working with the data.

Commented [MB7]: Line 260: Why use absolute salinity? The convention is to use PSU for data and data products, and do the conversion to absolute salinity in a second step working with the data.

Formatted: Superscript

Field Code Changed

calibration quality. In cruise 48UR20050412, which comprised two legs, discrete samples from only one leg were used for the entire cruise calibration, further affecting quality of the CTD-O₂ data. Figure 3c summarizes the cruise-level agreement using mean residuals and the percentage of residual values within ± 2 $\mu\text{mol/kg}$. Following Uchida et al. (2010), residuals within this threshold are considered acceptable. Cruises were categorized as follows: green: $\geq 40\%$ of residuals within ± 2 $\mu\text{mol/kg}$ (good agreement); blue: 19–39% of residuals within ± 2 $\mu\text{mol/kg}$ (moderate or uncertain agreement); grey: $< 19\%$ of residuals within ± 2 $\mu\text{mol/kg}$ (poor agreement and probably systematic bias in CTD-O₂ data). Eight cruises showed good agreement, eleven were moderate, and the remainder exhibited systematic positive or negative biases, as pointed by the mean value of the residuals (Figure 3c). These deviations may reflect sensor drift, post-calibration issues, or bottle-handling errors.



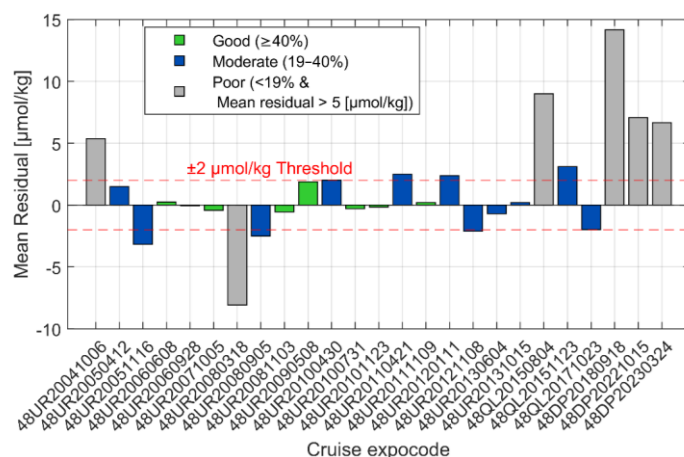


Figure 3. Residual values by cruise, showing the difference between CTD oxygen data (O_2 sensor) and Winkler oxygen data (O_2 bottle): (a) against pressure with each cruise identified with the starting date; (b) whisker plot with additional information about the % of data with residual values within $\pm 2 \mu\text{mol/kg}$ for each cruise identified with the expocode, and, (c) general assessment of each cruise, identified with the expocode, depending on the value of the mean residual and the % of residual values withing $\pm 2 \mu\text{mol/kg}$.

Table 1. Cruises contained in the CTD- O_2 WMED data product; for each cruise, the alias, expocode, research vessel and date information are provided, along with the number of stations with CTD- O_2 profiles (Nb). Refer to Table S1, Belgacem et al. (2020) and Ribotti et al. (2022) for additional cruise metadata.

Cruise ID	Cruise Alias	Expocode	Research Vessel (RV)	Date Start/End	Nb CTD profile
2	MEDGOOS9	48UR20041006	Urania	6 - 25 OCT 2004	82
3	MEDOC05/ MFSTEP2	48UR20050412	Urania	24 APR - 16 MAY 2005	160
5	MEDGOOS11	48UR20051116	Urania	16 NOV - 3 DEC 2005	36
6	MEDOC06	48UR20060608	Urania	8 JUN - 3 JUL 2006	127
8	MEDGOOS13/MEDBIO06	48UR20060928	Urania	28 SEP - 8 NOV 2006	41
9	MEDOC07	48UR20071005	Urania	5 - 29 OCT 2007	81
10	SESAMEIt4 KM3	48UR20080318	Urania	18 MAR - 7 APR 2008	27
11	SESAMEIT5	48UR20080905	Urania	5 - 16 SEP 2008	24
12	MEDCO08	48UR20081103	Urania	3 - 24 NOV 2008	60
13	TYRRMOUNTS	48UR20090508	Urania	8 MAY - 3 JUN 2009	86
14	BIOFUN010	48UR20100430	Urania	30 APR - 17 MAY 2010	29
15	VENUS1	48UR20100731	Urania	31 JUL - 25 AUG 2010	116
16	BONSIC2010	48UR20101123	Urania	23 NOV - 9 DEC 2010	24
17	EUROFLEET11	48UR20110421	Urania	21 APR - 8 MAY 2011	31
18	BONIFACIO2011	48UR20111109	Urania	9 - 23 NOV 2011	18
20	ICHNUSSA12	48UR20120111	Urania	11 - 27 JAN 2012	35
21	EUROFLEET2012	48UR20121108	Urania	8 - 26 NOV 2012	75
211	VENUS 2	48UR20130604	Urania	4 - 25 JUN 2013	59
22	ICHNUSSA13	48UR20131015	Urania	15 - 29 OCT 2013	40
222	ICHNUSSA15	48QL20151123	Minerva Uno	23 NOV - 14 DEC 2015	62
23	OCEANCERTAIN15	48QL20150804	Minerva Uno	4 - 18 AUG 2015	90
24	ICHNUSSA17/INFRAOCE17	48QL20171023	Minerva Uno	23 OCT - 28 NOV 2017	41
25	ICHNUSSA/JERICO18	48DP20180918	DallaPorta	18-25 SEP 2018	10
27	JERICO-II-2022	48DP20221015	DallaPorta	15- 25 OCT 2022	21
28	JERICO-III-EurogoShip-2023	48DP20230324	DallaPorta	24 MAR - 09 APR 2023	6

Formatted: Subscript

150 **3 Primary and secondary quality control methods**

151 **3.1 Reference cruises with Winkler dissolved oxygen data in the WMED**

152 An external reference data set for dissolved oxygen discrete measurements was used to compare the CNR CTD-

153 O₂WMED data. Discrete Winkler measurements on those reference cruises (Table 2, Figure 5~~4~~) were performed

154 following the GO-SHIP (Global Ocean Ship-Based Hydrographic Investigations Program) protocol ensuring

155 robust O₂ data quality to better than 1 µmol/kg (Langdon, 2010). Among these reference, cruises 06MT20011018

156 and 06MT20110405 are significant surveys, contributing to the GLODAPv2 data product (Olsen et al., 2016;

157 2020). They underwent full quality control with no bias correction applied to the original data. Similarly cruises

158 48UR20070528, 29AH20140426, and 06M220180302, which are being assembled into the consistent carbon and

159 ancillary dataset CARIMED (CARbon, tracer, and ancillary data In the MEDsea, Alvarez et al., 2019), have been

160 rigorously quality controlled (Álvarez et al., in preparation). ~~C~~The cruises 29AJ20160818 and 11BG20220517

161 conducted in 2016 and 2022 (Tanhua, 2019a, 2019b; Jullion, 2016; Schroeder, 2022; Schroeder et al., 2024)

162 followed GO-SHIP protocols under the Med-SHIP (Mediterranean Sea repeat hydrography) framework, which

163 emphasizes the collection of high-quality hydrographic and biogeochemical data for long-term climate studies

164 (Schroeder et al., 2015, 2024). These seven reference cruises were selected based on data quality and geographic

165 overlap with the CTD-O₂WMED dataset. Figures 1 and 5 shows the regional distribution of the reference data,

166 which aligns well with the CTD-O₂WMED cruise tracks, particularly in the Tyrrhenian Sea and Algeri~~ana~~ basin

167 which are the two most frequently sampled subregions.

168 **Table 2.** Overview of reference cruise datasets with high quality Winkler oxygen measurements, including

169 expocode. The dataset covers the period from 2001 to 2022.

Cruise Alias	EXPOCODE	Date starts and end	Stations	Source	Chief scientist(s)
<i>M51/2</i>	06MT20011018	18 Oct–11 Nov 2001	6	GLODAPv2	Wolfgang Roether
<i>TRANSMED_LEG II</i>					
	48UR20070528	28 May–12 Jun 2007	4	CARIMED	Maurizo Azzaro
<i>M84/3</i>	06MT20110405	5–28 Apr 2011	20	GLODAPv2	Toste Tanhua
<i>HOTMIX</i>	29AH20140426	26 Apr–31 May 2014	18	CARIMED	Javier Aristegui
<i>TAIPro-2016</i>	29AJ20160818	18–28 Aug 2016	42	Med-SHIP	Loïc Jullion
					Dagmar
<i>MSM72</i>	06M220180302	2 Mar–3 Apr 2018	130	GO-SHIP	Hainbucher
<i>TAIPro-2022</i>	11BG20220517	17–26 May 2022	24	Med-SHIP	Katrin Schroeder

Formatted: Outline numbered + Level: 1 + Numbering Style: 1, 2, 3, ... + Start at: 1 + Alignment: Left + Aligned at: 0 cm + Indent at: 0,63 cm

Formatted: Outline numbered + Level: 2 + Numbering Style: 1, 2, 3, ... + Start at: 1 + Alignment: Left + Aligned at: 0,63 cm + Indent at: 1,4 cm

Commented [SL8]: I think Figure 5 is now mentioned before Figure 4. This should be changed (reorganized)

Commented [SL9]: And received no bias correction?

(a)

(b)

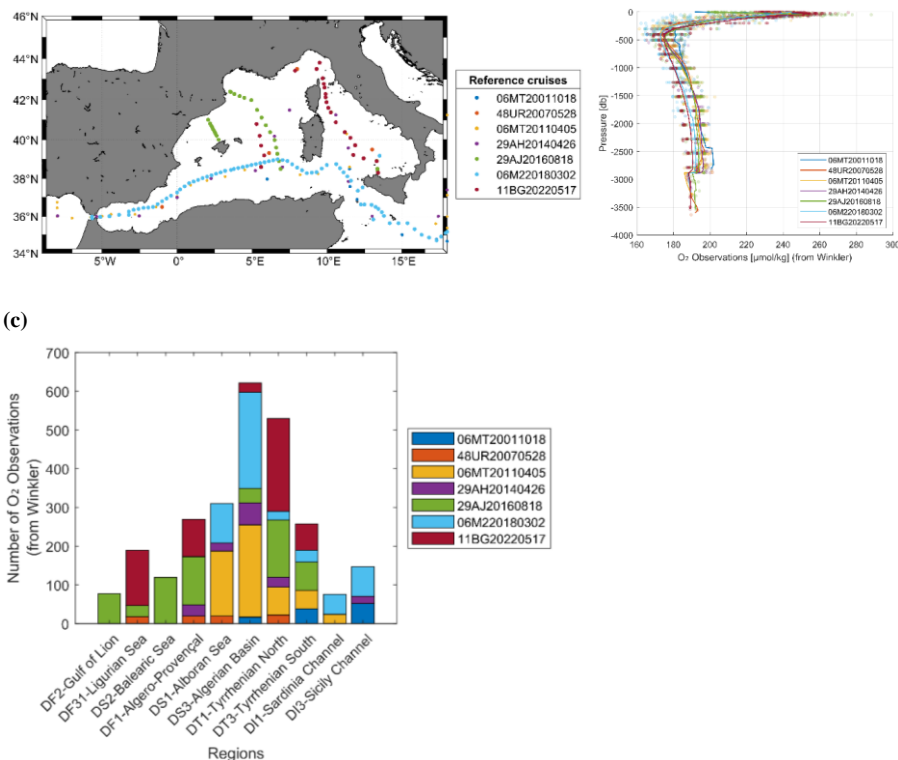


Figure 45. Reference cruises: (a) Map showing the location of reference stations; (b) vertical distribution of dissolved oxygen data from Winkler measurements, including the mean profile across all reference cruises; and (c) number of reference oxygen observations (Winkler measurements) per region.

3.2 Primary quality control of CTD-O₂ data

Following unit conversion and post-calibration with Winkler measurements (section 2.2), each cruise underwent an outlier screening process. Data quality flags were assigned following the WOCE standards: flag 2 for acceptable values, flag 3 for questionable values, flag 4 for bad values, and flag 9 for missing or not measured data. Flagging was tailored to the expected accuracy and precision of CTD-O₂ data for each individual cruise, which depends on the available measurements for Winkler oxygen and the stability of the CTD-O₂ sensor. Note that metadata information was scarce for some cruises. Property-property plots were analyzed for each region, and CTD-O₂ values identified as outliers in multiple plots were flagged as questionable. Approximately 0.2% of the CTD-O₂ data were flagged as outliers (flag 3). The 1st QC is inherently subjective, relying on the expertise of the analyst reviewing the data.

Formatted: Outline numbered + Level: 2 + Numbering Style: 1, 2, 3, ... + Start at: 1 + Alignment: Left + Aligned at: 0,63 cm + Indent at: 1,4 cm

Commented [SL10]: Even if you've not assigned any flag 4 it should be mentioned here that the flag exists

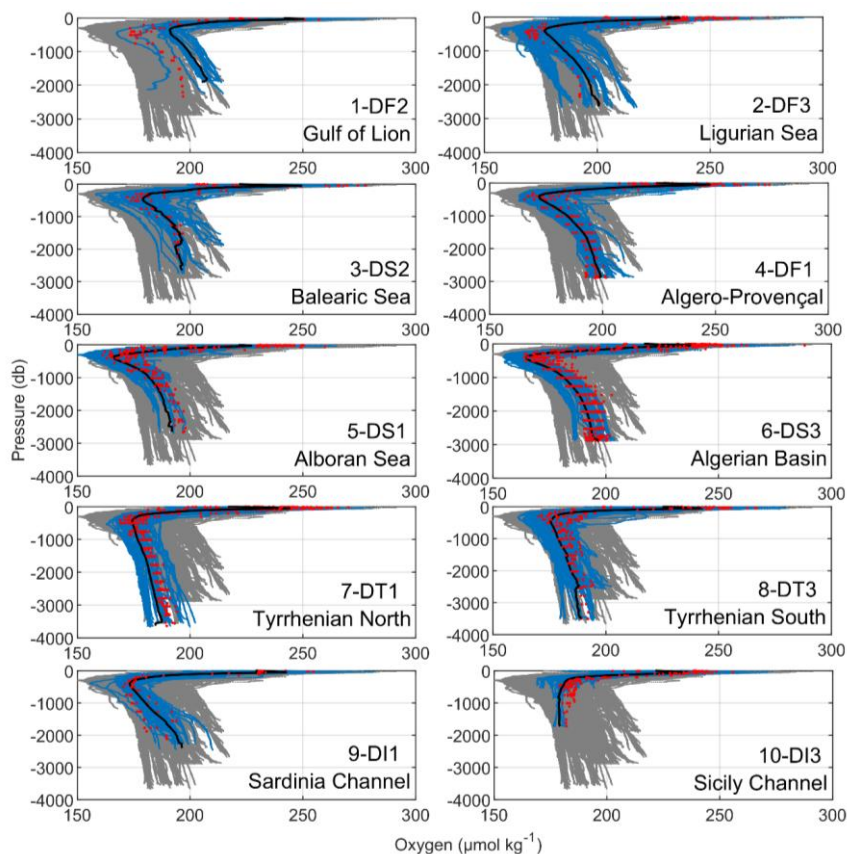
3.3 Overview and first assessment on CTD-O₂ WMED data

To illustrate the regional oxygen distribution, Figure 5.4a presents the vertical CTD-O₂WMED profiles by pressure across ten WMED subregions defined in Figure 4b-5b according to Manca et al. (2004). Gray lines show the full dataset, while blue lines indicates the range of oxygen concentrations in each subregion, revealing clear spatial and vertical patterns. The vertical distribution of dissolved oxygen in the WMED reflects a balance between air-sea gas exchange, biological activity, and regional circulation. Surface concentrations remain near atmospheric saturation due to gas exchange and photosynthesis activity. As organic matter sinks and is remineralized, oxygen is consumed at depth, generating vertical gradients. Unlike other ocean basins where pronounced OMZs develop, the WMED remain relatively well-oxygenated, thanks to episodic deep convection in the Gulf of Lion. This process ventilates the WMDW, which then spreads across subregions including the Algerian basin and Ligurian Sea, known to be among the best-ventilated areas (Schneider et al., 2014).

In the WMED, a recurrent feature is the intermediate OML, typically found between 300 and 600 db. This layer coincides with the core of the Eastern Intermediate Water (EIW), which is warmer, saltier, and consistently lower in oxygen than surrounding waters (Tanhua et al., 2013; Coppola et al., 2018; Mavropoulou et al., 2020). The OML's depth, thickness, and intensity vary by region and year, depending on remineralization rates, mixing, and circulation (Coppola et al., 2018). In the Tyrrhenian subregion (DT3, DT1), the oxygen increases again below the OML, suggesting the influence of deeper, more oxygenated waters. In contrast, the lowest oxygen levels in the WMED are found in the Sicily Channel (DI3) and Tyrrhenian Sea (DT3, DT1), where the EIW is prominent and deep ventilation is absent. The Alboran (DS1) and Balearic (DS2) Seas, by contrast, show relatively well-oxygenated profiles throughout the water column. This reflects both the presence of WMDW and enhanced vertical transport due to mesoscale and submesoscale processes that facilitate the downward movement of oxygen-rich surface waters (Middleton et al., 2025).

(a)

Formatted: Outline numbered + Level: 2 + Numbering
Style: 1, 2, 3, ... + Start at: 1 + Alignment: Left + Aligned
at: 0,63 cm + Indent at: 1,4 cm



(b)

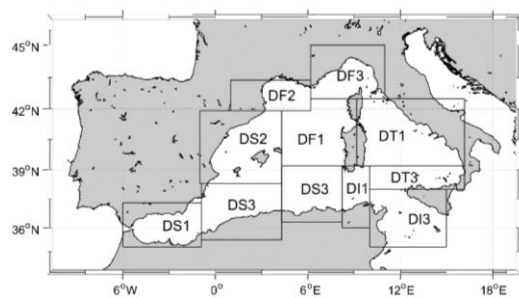


Figure 5. (a) Vertical distribution of CTD-O₂ (μmol/kg) versus pressure across the WMED. Grey profiles represent individual stations from the full dataset after initial quality control (1st QC). Blue shading shows the oxygen concentration envelope within each subregion (see Table S2), while black lines indicate the subregional mean profiles averaged over the entire period. Red dots represent selected reference profiles used for comparative analysis. (b) Map showing the geographic boundaries of the MEDAR/MEDATLAS subregions used in this study (see Table S2), adapted from Manca et al. (2004).

213

214 In order to assess the internal consistency and precision of the CTD-O₂WMED data across CNR cruises, we
215 computed for each cruise the median and median absolute deviation (MAD) of deep oxygen values flagged as
216 good (depth > 800 dbar, see Figure 6 and Table S3, in the Supplementary Material). This approach minimizes the
217 influence of atmospheric forcing, mesoscale variability and residual outliers. Figure 6a illustrates the spatial
218 variability in deep-water oxygen concentrations across the WMED. A pronounced east-west gradient is evident,
219 with lower oxygen levels (blue tones) in eastern subregions such as the Tyrrhenian Sea, Sardinia Channel, and
220 Sicily Channel, and higher oxygen levels (green to yellow) in western regions, where deep convection processes
221 in the Gulf of Lion enhance ventilation. The MAD was used as a proxy for precision, and overall MAD values
222 ranged from 0.1 to 7.5 $\mu\text{mol/kg}$. In well-sampled subregions (≥ 5 cruises) high MAD values or anomalous medians
223 were used to identify potentially biased CTD-O₂ cruises.

224 Below we summarize the findings by subregion:

- 225 - Ligurian Sea (DF3): of the five cruises, cruise #3 (48UR20050412) and #21 (48UR20121108) had the
226 highest MAD. Cruise #2 (48UR20041006) had a median consistent with the others, but cruise #3 was
227 $\sim 10 \mu\text{mol/kg}$ lower, and cruise #6 was $\sim 16 \mu\text{mol/kg}$ higher, despite a low MAD, suggesting possible
228 bias or calibration errors.
- 229 - Balearic Sea (DS2): among the six cruises, all but cruises #3 (48UR20050412) and #6 (48UR20060608)
230 showed low MAD values. Cruise #3 and #6 had MADs of 5.4 and 6.9 $\mu\text{mol/kg}$, respectively, indicating
231 lower precision.
- 232 - Algéro-Provençal region (DF1): ten cruises sampled this subregion. Cruise #24 (48QL20171023) showed
233 the highest MAD (7.5 $\mu\text{mol/kg}$) and the highest median, but was based on only two profiles which likely
234 explains the high uncertainty. Cruise #3 again exhibited an anomalously high median (197.6 $\mu\text{mol/kg}$),
235 and cruise #6 (48UR20060608) had a notably high MAD of 4.2 $\mu\text{mol/kg}$.
- 236 - Algerian basin (DS3): ten cruises generally agreed well (MAD: 1.8-4.1 $\mu\text{mol/kg}$). Cruise #22
237 (48UR20131015, carried out in 2013) had elevated oxygen concentrations that may reflect real increases
238 in deep oxygen. In contrast, cruise #3 (48UR20050412, carried out in 2005), showed a regionally high
239 median, suggesting possible data quality issues.
- 240 - Northern Tyrrhenian (DT1): among 14 cruises, MAD ranged from 1 to 4.5 $\mu\text{mol/kg}$. Cruises #3
241 (48UR20050412) and #222 (48QL20151123) had higher MAD values, with cruise #3 also showing a
242 high median, while cruise #2 (48UR20041006) recorded the lowest deep oxygen concentrations.
- 243 - Southern Tyrrhenian (DT3): the most frequently sampled region, with 20 cruises. MAD ranged from 0.1
244 and 5.3 $\mu\text{mol/kg}$. Elevated MAD values were observed for cruises #2 (48UR20041006), #3
245 (48UR20050412), #5 (48UR20051116), #6 (48UR20060608), #10 (48UR20080318), and #24
246 (48QL20171023), suggesting increased noise in the profiles.
- 247 - Sardinia Channel (DI1): fifteen cruises generally had consistent medians, though MAD values were
248 higher (3.5 to 6.5 $\mu\text{mol/kg}$). Recent cruises, particularly cruise #24 (48QL20171023), showed the highest
249 median (202.2 $\pm 6.3 \mu\text{mol/kg}$), significantly higher than earlier cruises, possibly indicating calibration
250 issues.

Commented [SL11]: Perhaps a formatting issue but I don't understand what range this is supposed to be

251 Following an approach adapted from Olsen et al. (2016), large MAD values, combined with anomalous medians
 252 and limited spatial coverage were used to identify cruises with low internal precision and potential systematic
 253 biases:

- 254 - Cruise #3 (48UR20050412), recurring multiple subregions, consistently showed high MAD or biased
 255 medians.
- 256 - Cruise #6 (48UR20060608) displayed unusually high medians (e.g., in DF3) and high MAD in DS2 and
 257 DT3.
- 258 - Cruise #24 (48QL20171023) (in DS3 and DT1) and cruise #22 (48UR20131015) exhibited elevated deep
 259 oxygen values and large MAD values, raising concerns about data quality or calibration.
- 260 - Cruise #2 (48UR20041006) (in DT1 and DT3) and cruise #5 (48UR20051116) showed both low median
 261 and high MAD a values, pointing to possible systematic error.

262 To support the regional assessment of data quality, a summary table (Table 3) compiles the number of cruises per
 263 subregion, highlights those with high MAD, and identifies cruises exhibiting anomalous median values. This table
 264 facilitates the identification of cruises with potential CTD-O₂ bias issues and helps assess the overall initial internal
 265 consistency of the CTD-O₂ dataset across the WMED.

266
 267

268 **Table 3.** Summary of CTD-O₂ Quality Control Results by Subregion

269

Subregion	Nb Cruises	Cruises with high MAD	Cruises with biased median	Notes
DF3 – Ligurian Sea	5	#3, #21	#3 (low), #6 (high)	Cruise #6 shows high values despite low MAD – potential calibration issue
DS2 – Balearic Sea	6	#3, #6	–	Both cruises show poor precision (high MAD)
DF1 – Algéro-Provençal	10	#24, #6	#3 (high), #24 (high)	#24 based on only 2 profiles; #6 and #3 raise concerns
DS3 – Algerian Basin	10	–	#3 (high), #22 (high)	#22 might reflect real signal; #3 likely biased
DT1 – Northern Tyrrhenian	14	#3, #222	#3 (high), #2 (low)	#2 and #3 indicate potential systematic errors
DT3 – Southern Tyrrhenian	20	#2, #3, #5, #6, #10, #24	#2 (low)	Frequent high MAD suggests noise or calibration issues
DII – Sardinia Channel	15	Most, esp. #24	#24 (high)	#24 significantly higher than earlier cruises – possible calibration bias

270

(a) (b)

Formatted: Caption

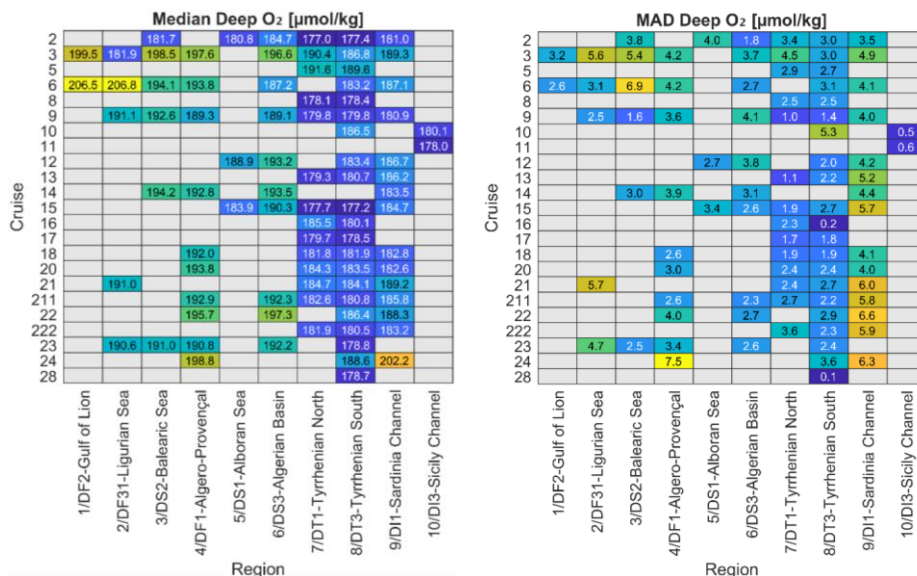


Figure 6. Median and median absolute deviation (MAD) of CTD-O₂WMED flagged as good data deeper than 800 dbar. Heatmaps show (a) the median and (b) MAD values, organized by cruise ID (rows) (Table 1) and geographic subregion (Figure 45) (columns). Grey cells indicate missing data. These metrics enable intercomparison of deep oxygen distribution and data quality across the CTD-O₂WMED dataset (Table S3). Color gradient: Blue to Green to Yellow indicate low to high values.

3.4 Secondary quality control procedure

The secondary quality control (2nd QC) procedure involves comparing the CTD-O₂ data from CNR cruises (Table 1) with selected reference cruises (Table 2). These reference datasets are assumed to be accurate and precise, with low temporal variability particularly in the deep ocean. However, this assumption may not fully hold for recent cruises due to strong spatial gradients and potential long-term trends in dissolved oxygen concentrations in the Mediterranean Sea.

Global synthesis efforts like [GLODAP](http://www.glodap.info) (www.glodap.info) (Key et al., 2004; Olsen et al., 2016,2019; Lauvset et al., 2024) and [CARINA](https://carina.euraxess.eu/) (Hoppema-Key et al., 2009|10) typically adopt a 1% threshold in crossover analysis to identify measurement biases and ensure inter-cruise consistency for oxygen. However, applying this same threshold to the Mediterranean may not be appropriate due to its unique oceanographic variability. Here, we assess the validity of reference cruise data, determine appropriate consistency thresholds, and identify the most temporally stable depth range for the crossover analysis in the WMED.

3.4.1. Threshold limit for dissolved oxygen data in the WMED

GLODAP applies a consistency or threshold limit for O₂ data of 1% as commented previously. However, given the natural variability in the Mediterranean Sea deep waters, we first assessed the appropriate threshold for crossover analysis by comparing the reference cruise data in two different regions, DS3 and DT1, two subregions with distinct deep-water dynamics. Winkler O₂ data from these reference cruises were interpolated to standard

Commented [MB12]: Table 5: What does the colors mean?

Formatted: Outline numbered + Level: 2 + Numbering Style: 1, 2, 3, ... + Start at: 1 + Alignment: Left + Aligned at: 0,63 cm + Indent at: 1,4 cm

Formatted: Hyperlink, Font: (Default) +Headings CS (Times New Roman), 10 pt, Complex Script Font: +Headings CS (Times New Roman), 10 pt, English (United States)

Field Code Changed

Commented [SL13]: I don't think hyperlinks are allowed. So Include the websites in parenthesis instead

Commented [SL14R13]: And include a reference for GLODAP here too

Commented [SL15]: I think Key et al (2010) is a better reference.

Key, R.M., Tanhua, T., Olsen, A., Hoppema, M., Jutterström, S., Schirnack, C., Van Heuven, S., Kozyr, A., Lin, X., Velo, A., Wallace, D.W.R., Mintrop, L., 2010. The CARINA data synthesis project: introduction and overview. Earth Syst. Sci. Data 2, 105-121. www.earth-syst-sci-data.net/2/105/2010/

Field Code Changed

Formatted: Outline numbered + Level: 3 + Numbering Style: 1, 2, 3, ... + Start at: 1 + Alignment: Left + Aligned at: 1,27 cm + Indent at: 2,16 cm

293 pressure intervals (0 - 3600 dbar) using a piecewise cubic Hermite interpolation to obtain station profiles. Then,
294 for each cruise and region, we calculated mean profiles (Figure 7).

295 The Algerian basin (region DS3, Figure 7a) exhibited a clear temporal variability. Deep (>1500 dbar) O_2 values
296 (>1500 dbar) in cruises from 2018 to 2022 were 4-5 $\mu\text{mol/kg}$ lower than those from earlier observations years –
297 a 2-4% deviation. These differences likely reflect reduced deep convection in recent years (Li and Tanhua, 2020;
298 Schneider et al., 2014), consistent with long-term observations and tracer-based studies.

299 Reference cruises 06M220180302 and 11BG20220517 in DS3 consistently report 2-4% lower deep O_2 levels
300 than compared to earlier cruises (e.g., 06MT20110405, 29AH20140426, 29AJ20160818) (See Figure S2),
301 corroborating the results in of Gregoire et al. (2023) and L. Coppola (pers. comm.), who linked the 2022 anomaly
302 to weakened deep convection.

303 In contrast, the Tyrrhenian Sea (region DT1, Figure 7b), on the other hand O_2 profiles between 800 and 2500
304 dbar were remarkably consistent across cruises, suggesting more temporally stable conditions in deep waters. This
305 is consistent with the region's known ventilation regime in the Tyrrhenian Sea, which is dominated by lateral
306 advection and double-diffusion rather than convection (Durante et., 2009). Small interannual variations, such as
307 the modest O_2 increases observed in 2007 and 2016, may reflect episodic ventilation events. These, and which
308 may also explain the weak influence the development of a well-defined tracer minimum zone (TMZ) in this
309 region the Tyrrhenian Sea (Li and Tanhua, 2020).

310 Figure 7c-d illustrate the variability of deep ocean O_2 concentrations in the WMED regions across cruises and
311 support adopting a 2% threshold to study the consistency of the CTD- O_2 WMED dataset in all subregions (Figure
312 S1-S2).

313

314

315

316

317

318

319

(a) DS3- Algerian basin

(b) DT1- Tyrrhenian Sea

Commented [MB16]: Line 227: "weak" ?

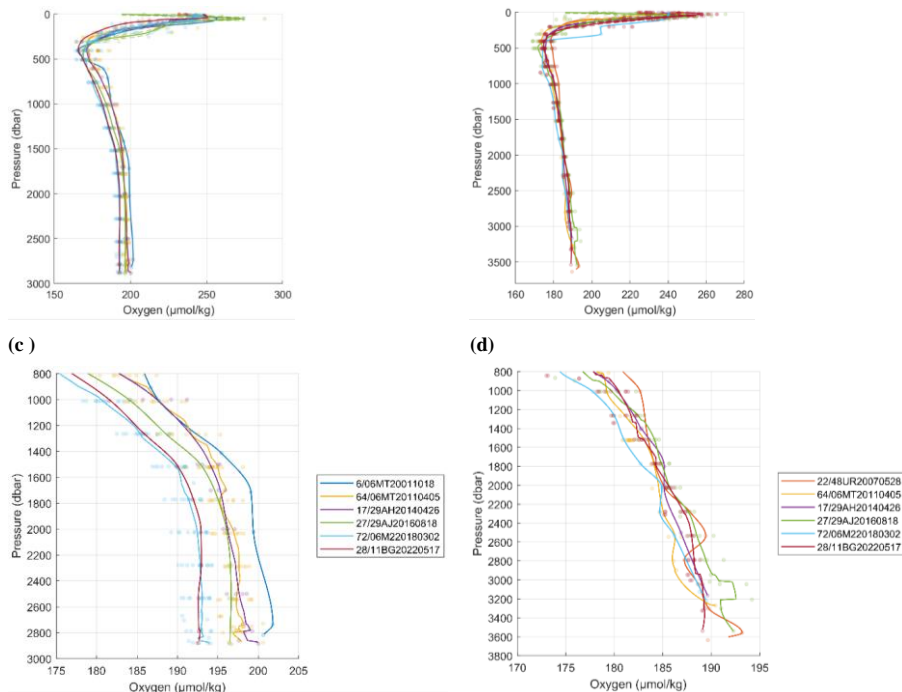


Figure 7. Average vertical profiles of dissolved oxygen in (a) the Algerian basin (region DS3) and (b) the Tyrrhenian Sea (region DT1). Panels (c) and (d) provide a zoomed view of the deep layers below 800 dbar. Colored dots represent discrete Winkler oxygen measurements, color-coded by cruise, while the solid-colored lines indicate cruise-specific mean profiles.

3.4.2. Defining a pressure range for the crossover analysis

The crossover results are evaluated in the water column region with the lowest temporal variability and lowest vertical gradient in terms of depth, density and/or potential temperature. Given the temporal changes in the Mediterranean Sea and particularly the WMED, we need to define our reference layer to evaluate the crossover results between cruises. Therefore, using the reference cruise O_2 data to determine the most stable depth range for crossover calculations, we computed pairwise ratios of mean profile O_2 values between the target reference cruise and other reference cruises in the subregion (e.g., $A/B = 06MT20011018 / \text{other reference cruises}$).

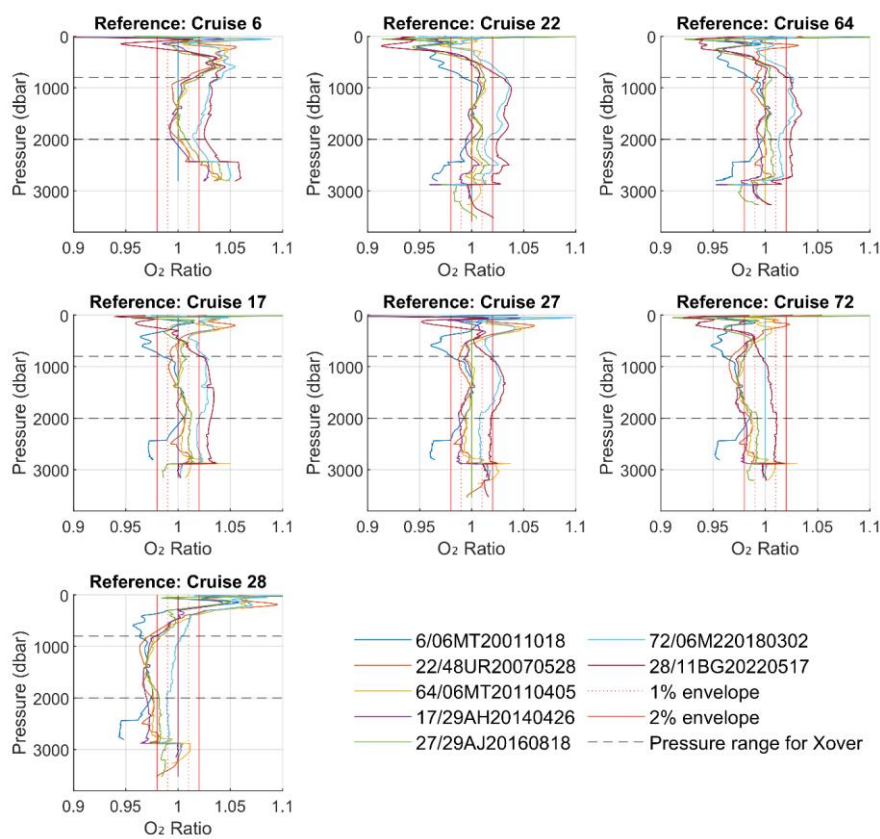
Results are shown in Figure 8 and Supplementary Figures S1-S2. As an overview, the results in Figure 8 clearly show that the deep and bottom waters in the WMED, below 2000 dbar, are not suitable to use as the most stable and reference layer, since here the data are sparse and natural variability increases.

Reference cruises 06M220180302 and 11BG20220517 in DS3 consistently report 2–4% lower deep O_2 levels than earlier cruises (e.g., 06MT20110405, 29AH20140426, 29AJ20160818), corroborating the results in Gregoire et al. (2023) and L. Coppola (pers. comm.), who linked the 2022 anomaly to weakened deep convection. Below 800 db, in the Algerian basin (region DS3), 29.7% of pairwise ratios fall within 1%, 60.5% within 2%, while 39% exceed the 2% threshold – indicating greater variability. In the Tyrrhenian Sea (region DT1), 71.7% of ratios fall within 1%, and 98.7% within 2% – confirming greater stability.

Formatted: Outline numbered + Level: 3 + Numbering Style: 1, 2, 3, ... + Start at: 1 + Alignment: Left + Aligned at: 1,27 cm + Indent at: 2,16 cm

Commented [SL17]: This seems more fitting in the previous section (on threshold limit). If it is relevant here you must at least specify which depth level(s) but in general I'd spend less time on the levels that are not relevant and more text on the levels that are relevant as reference. So if this is about the deep layers then I suggest you remove it and just refer to the figure above

340 The 800 – 2000 dbar range emerges as the most stable layer across cruises and regions and is selected as the
 341 reference one to evaluate the crossover analysis results. This layer corresponds with the TMZ described by Li and
 342 Tanhua (2020) and is less affected by long-term ventilation trends.



343 **Figure 8.** Vertical distribution of the ratio between mean dissolved oxygen profiles from Winkler discrete
 344 measurements for the reference cruises, each tested reference cruise (indicated at the top of each subplot) and the
 345 other reference cruises (listed in the legend box). The solid red vertical line marks the $\pm 2\%$ threshold limit, while
 346 the dashed red line indicates the $\pm 1\%$ threshold. Similar composite figures for subregions DT1 and DS3 are
 347 provided in the Supplementary Material (Figures S1 and S2, respectively), focusing on the 800-2000 dbar depth
 348 range.
 349

350 3.4.3. Crossover analysis

351 The crossover analysis was performed following Johnson et al. (2001) and Tanhua et al. (2011), taking advantage
 352 of the software tool provided in Lauvset and Tanhua (2015). CTD-O₂WMED cruises were compared with
 353 reference cruises by pairing stations within a 2° radius (~222 km). Interpolated profiles from each new cruise from
 354 CTD-O₂WMED (C1) were compared to those from the reference cruise (C2) within this distance. Each crossover
 355 comprises a minimum of three stations from each cruise where CTD-O₂ profiles were interpolated to standard
 356 density levels (sigma4) using Hermite interpolation. Using sigma4 as the vertical coordinate assures the

Formatted: Outline numbered + Level: 3 + Numbering
 Style: 1, 2, 3, ... + Start at: 1 + Alignment: Left + Aligned
 at: 1,27 cm + Indent at: 2,16 cm

Commented [SL18]: Above you mention A and B. Be
 consistent

comparison is made in the same water masses, thereby mitigating biases associated with variations in salinity. Mean difference profiles were computed at each crossover as the mean of different station pair differences, thus, one station in cruise C1 is compared to all stations in cruise C2, resulting in multiple mean difference profiles to finally calculate for each crossover pair the corresponding weighted mean and standard deviation profile, which are finally used to [determine](#) the weighted offset and standard deviation for the crossover pair. The weighting applied to the profiles is based on their variability, giving higher importance to parts of the profiles with lower variability (adapted from Tanhua et al., 2010, 2015). Figure 9 illustrates an example of a crossover pair and the corresponding offset between a CNR [cruise](#) and a reference cruise. The number of crossover stations is critical [because low sample sizes increase uncertainty](#): as illustrated in Figure 9a, 30 stations from C1 and 14 from C2 were compared ~~low sample sizes increase uncertainty~~. Additionally, while the number of crossover pairs is significant, the Mediterranean Sea has a limited number of reference cruises available. All calculated offsets for each cruise were [therefore](#) examined to determine the presence of any likely biases in the measurements.

In addition to the typical crossover analysis, we performed a regional crossover analysis using a simple modified clustering approach based on predefined WMED subregions (Table S2). Regional clusters included the Tyrrhenian Sea (DT1 and DT3), the Algerian basin (DS3 and DF1), and the Alboran Sea (DS1). [Clusters](#) were set manually by defining each subregion subsets following the geographical limits in table S2. This approach minimizes the impact of regional hydrographic differences.

374

375 3.4.4. Correction factors and final product consistency evaluation

For each cruise a set of offsets was obtained after the crossover analysis, and the corresponding inverse values are the Correction Factors (CF) which set the basis to obtain the final cruise CF for CTD-O₂ if needed. We applied a conservative approach: among the regional offsets, the CF closest to 1 (i.e., lowest absolute deviation) was selected (Table 3). This minimizes changes to the original data while improving internal consistency.

After applying the cruise CF, the final step involves evaluating the overall internal consistency of the CTD-O₂WMED dataset. This is done using the weighted mean (*WM*) which is calculated from the [absolute offsets \(*D*\)](#) across all crossovers (*L*) [after adjustment](#), weighted by the corresponding standard deviation (σ), following the approach described by Tanhua et al. (2009) and Belgacem et al. (2020).

$$384 \quad WM = \frac{\sum_{i=1}^L D(i) / (\sigma(i))^2}{\sum_{i=1}^L 1 / (\sigma(i))^2}$$

This assessment provides a quantitative measure of the internal coherence of the final data product, following earlier studies (Hoppema et al., 2009; Sabine et al., 2010; Tanhua et al., 2009). It is important to note that the evaluation is based on offsets relative to a selected reference dataset, under the assumption that these reference cruise data represent the [closest to the](#) trueness state of dissolved oxygen in the WMED.

Formatted: Outline numbered + Level: 3 + Numbering Style: 1, 2, 3, ... + Start at: 1 + Alignment: Left + Aligned at: 1,27 cm + Indent at: 2,16 cm

Commented [SL19]: After correction right?

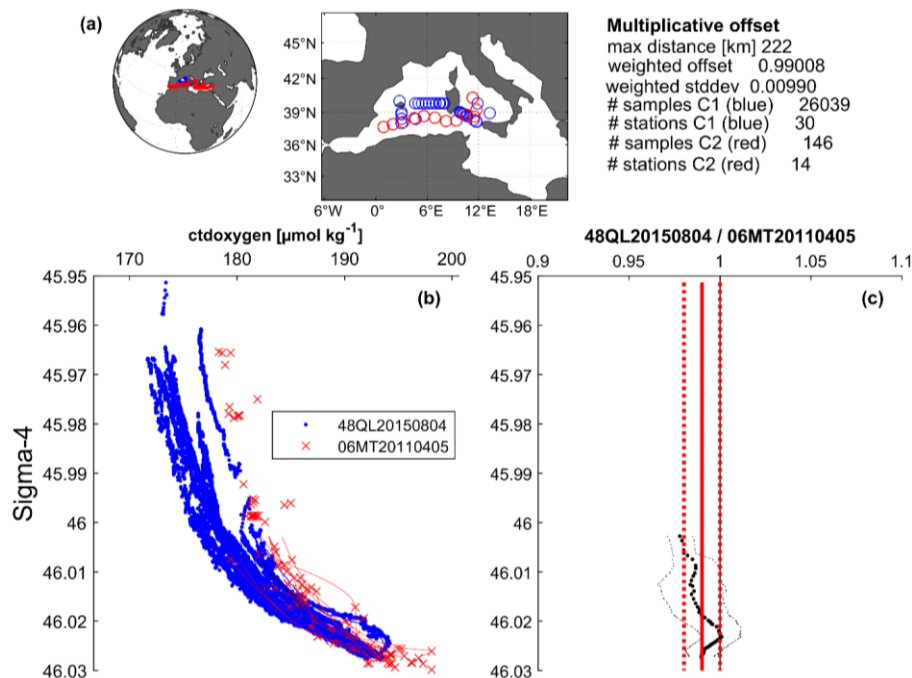


Figure 9. Example of a crossover pair analysis to obtain the offset ratio (multiplicative offset) in dissolved oxygen between cruise 48QL20150804 and the reference cruise 06MT20110405. (a) Spatial distribution of stations included in the crossover analysis: target cruise (blue) and reference cruise (red), with accompanying summary statistics. (b) Vertical profiles with sigma-t of dissolved oxygen ($\mu\text{mol/kg}$) from both cruises within a 2° radius and the 800 – 2000 dbar depth range. (c) Differences in dissolved oxygen between the two cruises: thick black dotted line shows the mean offset profile and the thin black dotted lines represent the standard deviation; the solid red line indicates the weighted average offset, and red dotted lines show the weighted standard deviation, values that are showed in the summary statistics in (a).

4 Secondary quality control results, correction factors to improve the CTD-O₂ WMED dataset

4.1 Overview of the secondary quality control results and impact on the CTD-O₂ WMED dataset

This section describes the obtained crossover results and discusses the ~~final~~-correction factor and the final adjustments applied, if needed, to each CNR WMED cruise, to finally probe the increased consistency of the CTD-O₂ WMED data product released. Each crossover result was evaluated, somehow subjectively, considering its quality, which would depend on the number of available stations, the calculated standard deviation of the offset, the depth range covered and the regional variability. A total of 265 crossover results for each cruise including regional clusters were carefully inspected and only the appropriate ones; following the conservative approach; were considered to obtain the correction factors (Figure 10). The final correction factors applied are summarized in Table 4 and only applied when the offset exceeded the $\pm 2\%$ threshold limit. Overall, only a few cruises exhibited deviations outside the $\pm 2\%$ limit, and thus required adjustments (Figure 10). The analysis indicated that deep oxygen values from cruises #2 (48UR20041006), #8 (48UR20060928), #211 (48UR20130604) and #222 (48QL20151123) required upward correction to align with the reference dataset. Conversely, cruises #3

Commented [SL20]: There are a few cases of this formatting error

Formatted: Outline numbered + Level: 1 + Numbering Style: 1, 2, 3, ... + Start at: 1 + Alignment: Left + Aligned at: 0 cm + Indent at: 0,63 cm

Commented [MB21]: line 803: Please be consistent in the language: I suggest using "adjustment" to what is applied to a cruise. So that table 3, it should be adjustments, assuming that those "suggested corrections" where actually applied.

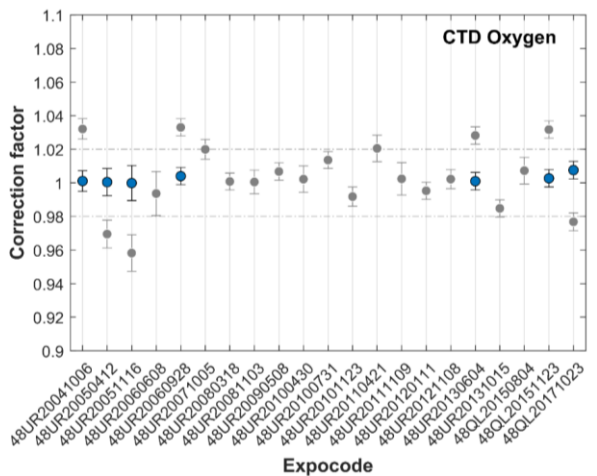
Formatted: Outline numbered + Level: 2 + Numbering Style: 1, 2, 3, ... + Start at: 1 + Alignment: Left + Aligned at: 0,63 cm + Indent at: 1,4 cm

Commented [SL22]: It might be worth to explain a bit more how "appropriate" is defined

411 (48UR20050412), #5 (48UR20051116), and #24 (48QL20171023) showed slightly higher values compared to their
412 respective reference and were adjusted downward. Fourteen cruises did not require any correction, as their values
413 were consistent with the reference dataset. **Cruises #25 (48DP20180918)**, #27 (48DP20221015), and #28
414 (48DP20230324) were excluded from the crossover analysis due to an insufficient number of deep stations below
415 800 dbar, but their data remain part of the final dataset. The reader is encouraged to compare the descriptions with
416 the corresponding plots in Figure 10 and the crossover summary figures in the Supplementary Material (Figures
417 S3 to ~~S7S9~~).
418 After applying the correction factors listed in Table 4, the offsets were recalculated to validate the adjustments. As
419 shown in Figure 10, the corrected values (in blue) reduced the recalculated offsets and improved consistency. To
420 assess the overall consistency of the adjusted CTD-O₂WMED dataset, we computed the WM of the crossover
421 offsets after ~~correction adjustments~~ (Figure 11). The internal consistency of the final CTD-O₂WMED dataset was
422 estimated at 0.998. These adjustments reduced potential biases linked to errors related to methodological
423 discrepancies, resulting in improved coherence across the dataset.

Formatted: Highlight

Formatted: Highlight



424
425 **Figure 10.** Results of the crossover analysis for CTD dissolved oxygen, showing the recommended correction
426 factors before (grey) and after (blue) adjustment (i.e., after applying the correction ~~factor~~). Error bars represent the
427 standard deviation of the absolute weighted offset. Corrections indicate the multiplicative factor to be applied to
428 the original CTD oxygen data (see Table ~~43~~). The dashed line marks the $\pm 2\%$ threshold limit of adjustment.

429 **Table 4.** Summary of the recommended multiplicative correction factors for the CTD-O₂WMED cruises derived
430 from the 2nd QC procedure.

Cruise ID	EXPOCODE	Correction factor
		Ajustements
2	48UR20041006	1.032
3	48UR20050412	0.97
5	48UR20051116	0.96
6	48UR20060608	-
8	48UR20060928	1.03
9	48UR20071005	-
10	48UR20080318	-
11 + 12 ^a	48UR20080905	-
	+ 48UR20081103	-

Commented [SL23]: There is an inconsistent use of significant figures in this table.

Commented [MB24]: ine 803: Please be consistent in the language: I suggest using "adjustment" to what is applied to a cruise. So that table 3, it should be adjustments, assuming that those "suggested corrections" where actually applied.

13	48UR20090508	-
14	48UR20100430	-
15	48UR20100731	-
16	48UR20101123	-
17	48UR20110421	-
18	48UR20111109	-
20	48UR20120111	-
21	48UR20121108	-
211	48UR20130604	1.028
22	48UR20131015	-
222	48QL20151123	1.03
23	48QL20150804	-
24	48QL20171023	0.97

^aCruise #11 and cruise #12 were merged in the 2nd QC.

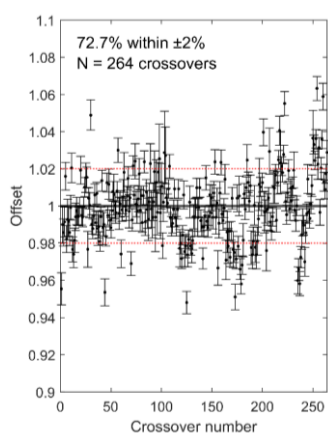


Figure 11. Crossover results showing the weighted mean offset and standard deviation for the CTD-O₂WMED cruises after applying the correction factors. The dashed red line marks the $\pm 2\%$ threshold.

4.2 Detailed description of each CNR WMED cruise corrected

This subsection provides a rationale for the proposed correction factors in Table 4. It includes interpretations of significant offsets, even in cases where no final correction was applied but poor data quality was observed. Cruises not mentioned below were found to be consistent with the reference data and required no further review.

- Cruise#2 (48UR20041006): Two C_{crossovers} were found in the Alboran Sea-(2), five in the Algerian basin (5), and four in the Tyrrhenian Sea-(4). A consistent mean offset of 0.96 ± 0.005 across all regions suggests CTD-O₂ values were $\sim 4\%$ lower than the reference cruises (Figure 12). This is also supported by high residuals between Winkler and sensor data ($>2 \mu\text{mol/kg}$, Figure 3) and by the unusually low regional deep averages (Figure 65). Given that deep WMED ventilation prior to 2004 was still stable, a 3.2% increase. An adjustment of (a correction factor of 1.032) is recommended applied.

Commented [SL25]: You should go through this section and make sure you are consistent in how many significant figures, or decimal places, you give for the correction factors and percentages. Right now there are inconsistencies and they are not explained

Formatted: Outline numbered + Level: 2 + Numbering Style: 1, 2, 3, ... + Start at: 1 + Alignment: Left + Aligned at: 0,63 cm + Indent at: 1,4 cm

Commented [MB26]: Line 838: Did you apply the adjustment? I suggest using the term adjustment to what is actually applied to the data product. For each of the descriptions of the individual cruises, end by stating what adjustment was applied based on the evidence you provide.

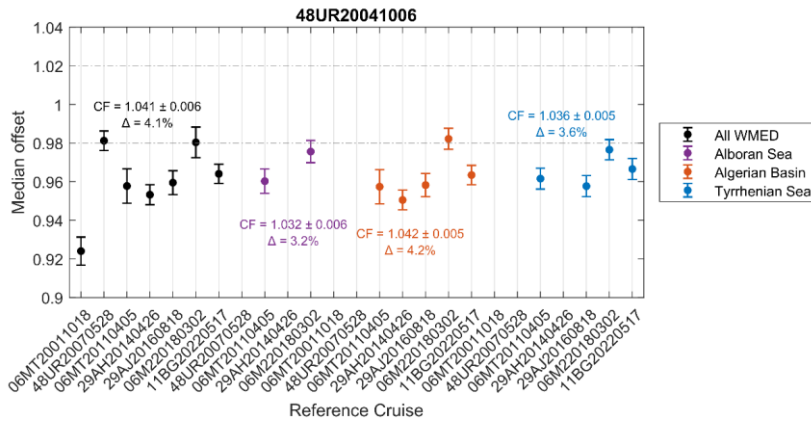


Figure 12. Summary of CTD-O₂ crossover results for cruise #2 (48UR20041006) relative to the reference cruises showed along the x-axis arranged chronologically. Dashed grey lines indicate the $\pm 2\%$ threshold. Black dots with error bars represent the weighted mean offsets and corresponding weighted standard deviation. Colored markers denote the subregions: purple for the Alboran Sea, orange for the Algerian basin, and blue for the Tyrrhenian Sea. Annotated within the figure are the correction factor, standard deviation, and percentage change of the median offsets for each subregion.

- Cruise #3 (48UR20050412): this cruise has five crossovers in the Algerian basin and four in the Tyrrhenian Sea clearly indicating the need for a downward adjustment. As pointed out in section 3.4.3, this cruise could be of low precision compared to cruises conducted in the same regions. Based on the agreement between the offsets in both subregions (Figure 13), and despite one reference cruise in (2001) suggested agreement (but it involved only three stations, therefore it is not robust). An overall offset of 1.03 ± 0.008 was found, supporting a correction factor adjustment of 0.97 (-3%).

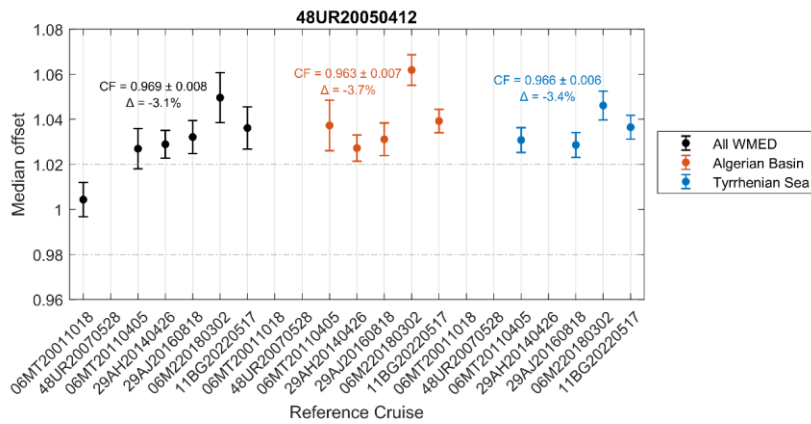


Figure 13. Same as Figure 12 but for cruise #3 (48UR20050412).

- Cruise #5 (48UR20051116): four crossovers in the Tyrrhenian Sea spanning the years 2011, 2016, 2018 and 2022 (Figure S3) showed good agreement (weighted standard deviation of 0.01), but a median weighted offset of 1.042 ± 0.01 . The suggested correction factor is 0.96 ($\sim -4.2\%$ lower). The quite large discrepancy may indicate potential issues with the sensor (section 3.3, Table 3). An adjustment of 0.96 is applied;
- Cruise #6 (48UR20060608): five crossovers in the Algerian basin and four in the Tyrrhenian Sea (Figure 14S.4). While offsets seem to increase over time, seven of nine crossovers were lower than $\pm 2\%$. The Tyrrhenian Sea, a quite stable region for deep waters, showed low variability (weighted standard deviation of 0.005), indicating a good precision and good agreement between crossovers. The Algerian basin was more variable and represented the direct effect of the Gulf on Lion (where deep-water convection may occur). Here, the weighted standard deviation was higher (~ 0.01), persistent in all references except for the 2022 reference. Given the lack of consistency between subregions and trends similar to reference profiles (Figure 7c), no correction-adjustment is applied.

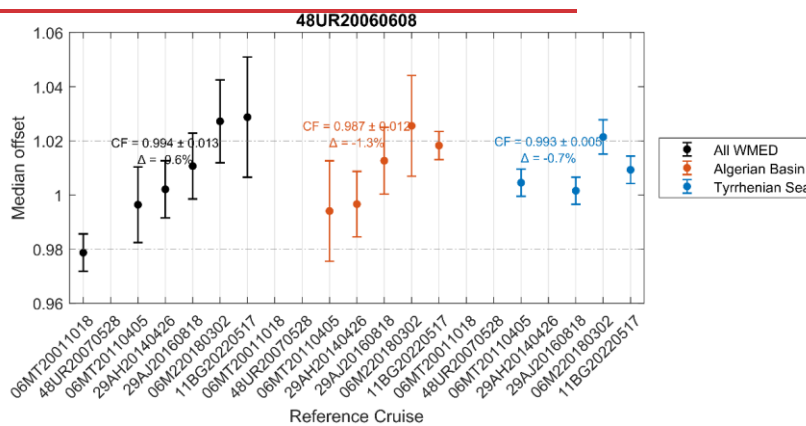


Figure 14. Same as Figure 12 but for cruise #6 (48UR20060608).

- Cruise #8 (48UR20060928): four crossovers in the Tyrrhenian Sea showed good agreement (weighted standard deviation of 0.005), with reference cruises 06MT20110405, 29AJ20160818, 06M220180302 and 11BG20220517 (Figure S4S5). Offsets were found to be between 0.96 ± 0.005 and 0.97 ± 0.005 , and an increase of $+3\%$ is recommended. And adjustment-correction factor of 1.03 is applied, recommended ($+3\%$).
- Cruise #9 (48UR20071005): crossovers in both the Algerian basin (5) and Tyrrhenian Sea (4) showed consistent offsets of 0.97 ± 0.01 – 0.98 ± 0.005 , indicative of the good precision of the data. The largest offset (0.95 ± 0.005) occurred with reference cruise 06MT20011018 (Figure 15.14), likely due to limited station coverage. Both subregions show a consistent deviation about $+2\%$ but as all values remain within the $\pm 2\%$ limit no adjustment is recommended.

Formatted: Font: (Default) +Headings CS (Times New Roman), 10 pt, Complex Script Font: +Headings CS (Times New Roman), 10 pt

Formatted: Font: (Default) +Headings CS (Times New Roman), 10 pt, Complex Script Font: +Headings CS (Times New Roman), 10 pt

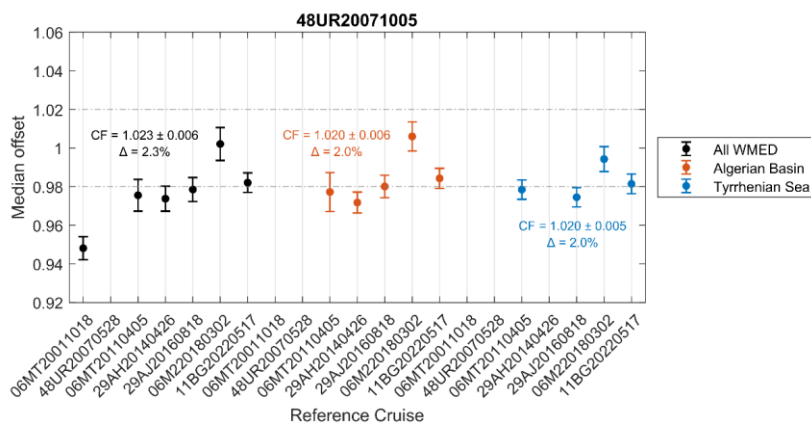


Figure 1415. Same as Figure 12 but for cruise #9 (48UR20071005).

- Cruise #15 (48UR20100731): two crossovers in the Alboran Sea with a median offset of 0.98 ± 0.01 , five crossovers in the Algerian basin with an offset of 0.98 ± 0.005 , and four crossovers in the Tyrrhenian Sea showing an offset of 0.97 ± 0.005 (Figure 146S6). Following our conservative correction approach, the lowest observed percentage of change is 1.4% in the Algerian basin, suggesting a correction factor of 1.014, below the $\pm 2\%$ threshold limit. Therefore, no adjustment is applied.

Formatted: Justified

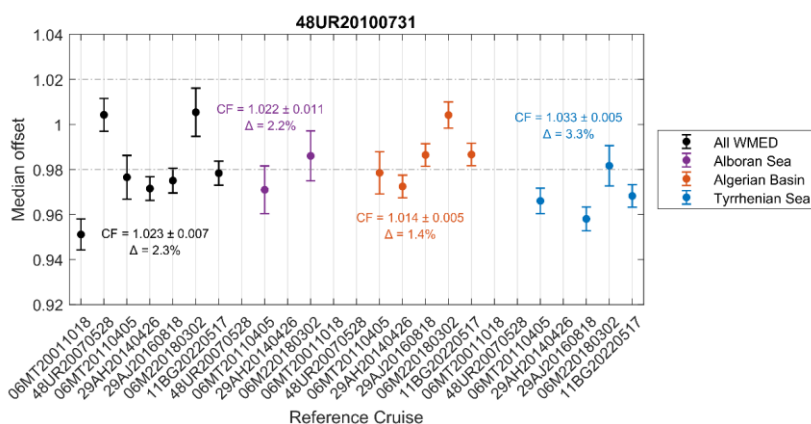


Figure 16. Same as Figure 12 but for cruise #15 (48UR20100731).

- Cruise #211 (48UR20130604): the crossovers suggest a 6% increase in the Algerian basin and 2.8% in the Tyrrhenian Sea (Figure 175). Both median offsets indicate that oxygen data for this cruise are lower than the references, although data precision appears good. Despite the regional difference and following our conservative approach, we recommend applying an increase of +2.8%, prioritizing the smaller offset to avoid overcorrection. An adjustment of 1.028 is applied.

- Cruise #22 (48UR20131015): this cruise was carried out in the same year as cruise #211 (48UR20130604), but shows smaller offsets in both regions (Algerian basin and Tyrrhenian Sea) (Figure S5S7), suggesting its oxygen values are higher than the references and might require a small downward correction adjustment of -1.5%, that - However, the recommended correction factor of 0.98 ± 0.005 in both regions is within the $\pm 2\%$ limit. No adjustment is applied.

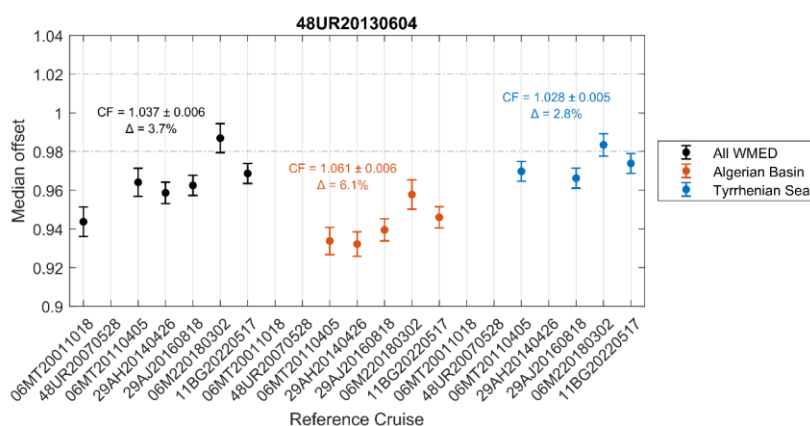


Figure 1517. Same as Figure 12 but for cruise #211 (48UR20130604).

- Cruise #222 (48QL20151123): four crossovers in the Tyrrhenian Sea, spanning multiple years (Figure S6S8), indicated a consistent underestimation of CTD-O₂ data (offset 0.97 ± 0.005). The data exhibit good precision, with a weighted standard deviation of 0.005. An correction factor of 1.03% is recommended. A final adjustment of 1.03 is applied.
- Cruise #24 (48QL20171023): four Tyrrhenian Sea crossovers in the Tyrrhenian Sea (Figure S97) show CTD-O₂ values slightly higher than the reference cruises. The median offset suggests a decrease of approximately 3%, indicating a correction factor of 0.97.
- To resume, the CTD-O₂WMED original version includes all cruises that has passed the first levels of quality checks, but has not yet been corrected through crossover analysis (i.e., secondary quality control), so no adjustments were applied the original version. However, the adjusted version of the dataset CTD-O₂WMED-adjusted builds upon the original dataset by incorporating the secondary quality control adjustments.

5 Summary and conclusions

This study aimed to evaluate and enhance the consistency of a collection of CTD-O₂ measurements of 25 cruises in the WMED with a relevant CNR Italian participation. A 1st quality control was applied followed by a secondary quality control procedure based on crossover analysis was adapted to the specificizes of the dataset and the WMED: the threshold limit was increased from 1% to 2% recognizing the limitations in terms of accuracy and

Formatted: Font: (Default) +Headings CS (Times New Roman), 10 pt, Complex Script Font: +Headings CS (Times New Roman), 10 pt

Formatted: Font: (Default) +Headings CS (Times New Roman), 10 pt, Complex Script Font: +Headings CS (Times New Roman), 10 pt

Formatted: Font: (Default) +Headings CS (Times New Roman), 10 pt, Complex Script Font: +Headings CS (Times New Roman), 10 pt, English (United States)

Formatted: Font:

Formatted: Font: (Default) +Headings CS (Times New Roman), 10 pt, Complex Script Font: +Headings CS (Times New Roman), 10 pt

Formatted: Normal, Indent: Before: 0,63 cm, No bullets or numbering

Formatted: Font: (Default) +Headings CS (Times New Roman), 10 pt, Complex Script Font: +Headings CS (Times New Roman), 10 pt

Formatted: Outline numbered + Level: 1 + Numbering Style: 1, 2, 3, ... + Start at: 1 + Alignment: Left + Aligned at: 0 cm + Indent at: 0,63 cm

Formatted: Superscript

529 precision of our dataset and the known temporal variability in some WMED basins; and we determined it is more
530 appropriate to study the consistency of CTD-O₂ data in the 800-2000 dbar layer rather than the deep and bottom
531 waters which are much more variable. The methodology developed here provides a robust and transferable
532 framework for quality control in regions with similarly complex hydrography.

533 The 2nd QC procedure obtained a total of 265 crossover comparisons between the CTD-O₂ data and Winkler
534 measurements from a selection of reference cruises following GO-SHIP procedures, with a higher precision and
535 accuracy. While the majority of checked CTD-O₂ cruise data fell within the $\pm 2\%$ limit, a limited number showed
536 systematic offsets that warranted correction. Adjustments were applied conservatively—only when deviations
537 exceeded the defined threshold and using the smallest possible correction factor. ~~Corrections~~ ~~Adjustments~~ were
538 recommended for seven cruises. Although these cruises are categorized as moderate in quality, they are retained
539 in the final dataset as ~~corrected-adjusted~~ data. A few cruises ([#25 \(48DP20180918\)](#), [#27 \(48DP20221015\)](#), and
540 [#28 \(48DP20230324\)](#)) were excluded from the crossover analysis due to insufficient deep profiles but remain part
541 of the final dataset. The corrections led to a measurable improvement in the internal consistency of CTD-O₂ data
542 among cruises, as demonstrated by the weighted mean global offset of 0.998 calculated from post-adjustment
543 crossover analysis.

544 The CTD-O₂WMED original and corrected dataset is openly accessible to the scientific community through open
545 access repositories. Our product, despite limitations in temporal coverage, will substantially increase the
546 availability and reliability of dissolved oxygen data for long-term studies in the WMED. It builds upon and
547 complements earlier efforts in the region (Schneider et al., 2014; Coppola et al., 2017; Macías et al., 2018b;
548 Mavropoulou et al., 2020; Li and Tanhua, 2020; Cossarini et al., 2021; Friedland et al., 2021; Ulses et al., 2021;
549 Belgacem et al., 2019, 2020). Recent advances in numerical modeling (Reale et al., 2021), machine learning
550 (Fourrier et al., 2022), and autonomous platforms such as BGC-Argo floats and gliders in the WMED demand
551 measurements to validate their results. The CTD-O₂WMED dataset, in synergy with these emerging observation
552 systems, provides a valuable foundation for assessing changes in the regional oxygen budget and it will support
553 ongoing efforts to understand the WMED's response to climate-driven oceanographic changes and improve future
554 projections.

555 6 Data availability

556 The CTD-O₂WMED dataset (Belgacem et al., 2024 [in review], see temporary link below) is available at
557 PANGAEA (original: <https://doi.pangaea.de/10.1594/PANGAEA.974725> and Adjusted:
558 <https://doi.pangaea.de/10.1594/PANGAEA.982858>)

559 Table 5 shows the variables included in the dataset, which is composed in two parts:

- 560 - the first includes the aggregation of cruise data prior to correction, which has undergone calibration and
561 first-level quality check.
- 562 - the second contains the adjusted data product, incorporating the recommended corrections from the
563 secondary quality control procedure.

Commented [SL27]: Are these somehow flagged (similar to what GLODAP does)?

Formatted: Highlight

Commented [SL28]: You should include your own work on nutrients in this list

Formatted: Outline numbered + Level: 1 + Numbering Style: 1, 2, 3, ... + Start at: 1 + Alignment: Left + Aligned at: 0 cm + Indent at: 0,63 cm

Field Code Changed

Field Code Changed

Formatted: Font: (Default) +Headings CS (Times New Roman), 10 pt, Complex Script Font: +Headings CS (Times New Roman), 10 pt

564 The CTD-O₂WMED is complementary to the data product CNR-DIN-WMED available
565 <https://doi.org/10.1594/PANGAEA.904172>.

566 No special software is required to access the data. Note that data from the reference cruises used for crossover
567 analysis are not included in the final product (see Table 6).

568 06MT20011018 : <https://cehdo.uesd.edu/cruise/06MT20011018>

569 48UR20070528: (CARbon, tracer, and ancillary data In the MEDsea, Alvarez et al., 2019

570 <https://www.ncei.noaa.gov/archive/archive-management-system/OAS/bin/prd/iquery/accession/details/218462>

571 06MT20110405 : <https://cehdo.uesd.edu/cruise/06MT20110405>

572 29AH20140426 : [https://catalog.data.gov/dataset/dissolved-inorganic-carbon-dic-total-alkalinity-ph-on-total-scale-](https://catalog.data.gov/dataset/dissolved-inorganic-carbon-dic-total-alkalinity-ph-on-total-scale-chlorofluorocarbon-12-efc-12-3)
573 [chlorofluorocarbon-12-efc-12-3](https://catalog.data.gov/dataset/dissolved-inorganic-carbon-dic-total-alkalinity-ph-on-total-scale-chlorofluorocarbon-12-efc-12-3)

574 (CARbon, tracer, and ancillary data In the MEDsea, Alvarez et al., 2019

575 29AJ20160818 : <https://cehdo.uesd.edu/cruise/29AJ20160818>

576 06M220180302 : <https://cehdo.uesd.edu/cruise/06M220180302>

577 11BG20220517 : <https://cehdo.uesd.edu/cruise/11BG20220517>

578

579

580

581

582

583 **Table 5. Summary of data product parameters and units. List of parameters for the CTD-O₂WMED**
584 **dataset for both original and adjusted versions.**

Data Product	Parameter Name	Units
Parameter Name		
EXPOCODE	expedition code	
CRUISE	cruise number	
STATION	profile number	
CRUISE_ID	cruise id	
DAY	day	
MONTH	month	
YEAR	year	
LONGITUDE	longitude	decimal degrees [DEGREES EAST]
LATITUDE	latitude	decimal degrees [DEGRES NORTH]
CTDPRS	CTD pressure	decibars [DBAR]
DEPTH	depth	meters [M]
CTDSAL	CTD salinity	[PSS-78]
CTDSAL_FLAG_W	CTD salinity flag	
CTDTMP	CTD temperature	degrees C [ITS-90]
CTDOXY	CTD oxygen	micromole/kg [UMOL/KG]
CTDOXY_FLAG_W	CTD oxygen flag	

585

586

587 [Table 6. Reference dataset availability](#)

Field Code Changed

Commented [SL29]: It is probably smart to list the access points to the reference data here too

Formatted: English (United States)

Field Code Changed

Field Code Changed

Field Code Changed

Field Code Changed

Field Code Changed

Formatted: Font: (Default) +Headings CS (Times New Roman), 10 pt, Bold, Not Italic, Font color: Auto, Complex Script Font: +Headings CS (Times New Roman), 10 pt, Bold, Not Italic

Formatted: Font: (Default) +Headings CS (Times New Roman), 9 pt, Complex Script Font: +Headings CS (Times New Roman), 9 pt

Formatted Table

Formatted: Font: (Default) +Headings CS (Times New Roman), 9 pt, Complex Script Font: +Headings CS (Times New Roman), 9 pt, French (France)

Formatted: Font: (Default) +Headings CS (Times New Roman), 9 pt, Complex Script Font: +Headings CS (Times New Roman), 9 pt

Formatted: Font: (Default) +Headings CS (Times New Roman), 9 pt, Complex Script Font: +Headings CS (Times New Roman), 9 pt

Formatted: Font: (Default) +Headings CS (Times New Roman), 9 pt, Complex Script Font: +Headings CS (Times New Roman), 9 pt

Formatted: Font: (Default) +Headings CS (Times New Roman), 9 pt, Complex Script Font: +Headings CS (Times New Roman), 9 pt

Formatted: Font: (Default) +Headings CS (Times New Roman), 9 pt, Complex Script Font: +Headings CS (Times New Roman), 9 pt

Formatted

Formatted

Formatted

Formatted

Formatted

Formatted

Formatted

Formatted

Formatted

Formatted

Formatted

Formatted

608 sea, without them, this work would not have been possible. We also thank the Principal Investigators of the cruises
609 (Stefano Cozzi, Gabriella Cerrati, Stefano Aliani, Mario Astraldi, Maurizo Azzaro, Alberto Ribotti, Massimiliano
610 Dibitetto, Gian Pietro Gasparini, Annalisa Griffa, Jeff Haun, Loïc Jullion, Gina La Spada, Elena Mannini, Angelo
611 Perilli and Chiara Santinelli).

612

613

614

615

616 **References**

617 Álvarez, M., Sanleón-Bartolomé, H., Tanhua, T., Mintrop, L., Luchetta, A., Cantoni, C., Schroeder, K., and
618 Civitarese, G.: The CO₂ system in the Mediterranean Sea: a basin wide perspective, *Ocean Sci.*, 10, 69–92,
619 <https://doi.org/10.5194/os-10-69-2014>, 2014.

620 Álvarez, M., Catalá, T. S., Civitarese, G., Coppola, L., Hassoun, A. E. R., Ibello, V., Lazzari, P., Lefevre, D.,
621 Marcias, D., Santinelli, C., and Ulses, C: Chapter 11–Mediterranean Sea general biogeochemistry, Editor (s):
622 Katrin Schroeder, Jacopo Chiggiato, *Oceanography of the Mediterranean Sea*, [https://doi.org/10.1016/B978-0-12-](https://doi.org/10.1016/B978-0-12-823692-5.00004-2)
623 [823692-5.00004-2](https://doi.org/10.1016/B978-0-12-823692-5.00004-2), 2022.

624 Álvarez, M., Velo, A., Tanhua, T., Key, R., Heuven, S. V.: Carbon, tracer and ancillary data in the medsea,
625 carimed: an internally consistent data product for the ~~mediterranean~~-Mediterranean sea. Tech. Rep. 2019,
626 Instituto Español de Oceanografía, 2019.

627 Belgacem, M., Chiggiato, J., Borghini, M., Pavoni, B., Cerrati, G., Acri, F; Cozzi, S., Ribotti, A., Álvarez, M.,
628 Lauvset, S. K., and Schroeder, K.: Quality controlled dataset of dissolved inorganic nutrients in the western
629 Mediterranean Sea (2004– 2017) from R/V oceanographic cruises, PANGAEA [data set],
630 <https://doi.org/10.1594/PANGAEA.904172>, 2019.

631 Belgacem, M., Chiggiato, J., Borghini, M., Pavoni, B., Cerrati, G., Acri, F., Cozzi, S., Ribotti, A., Álvarez, M.,
632 Lauvset, S. K., and Schroeder, K.: Dissolved inorganic nutrients in the western Mediterranean Sea (2004–2017),
633 *Earth Syst. Sci. Data*, 12, 1985–2011, <https://doi.org/10.5194/essd-12-1985-2020>, 2020.

634 Belgacem, M., Schroeder, K., Lauvset, S. K., Álvarez, M., Chiggiato, J., Borghini, M., Cantoni, C., Ciuffardi, T.,
635 Sparnocchia, S.: O2WMED: Quality controlled dataset of dissolved oxygen in the western Mediterranean Sea
636 (2004-2023) from R/V oceanographic cruises [dataset], PANGAEA, in review: temporary link: [https://cnrsc-](https://cnrsc-my.sharepoint.com/:f/g/personal/malekbelgacem_cnr_it/EkIgo958UMlBmJ8SGwNB4HwBBX-FzDa8NI9C3vHeS4Vd4Q?e=Wt8p1I)
637 [my.sharepoint.com/:f/g/personal/malekbelgacem_cnr_it/EkIgo958UMlBmJ8SGwNB4HwBBX-](https://cnrsc-my.sharepoint.com/:f/g/personal/malekbelgacem_cnr_it/EkIgo958UMlBmJ8SGwNB4HwBBX-FzDa8NI9C3vHeS4Vd4Q?e=Wt8p1I)
638 [FzDa8NI9C3vHeS4Vd4Q?e=Wt8p1I](https://cnrsc-my.sharepoint.com/:f/g/personal/malekbelgacem_cnr_it/EkIgo958UMlBmJ8SGwNB4HwBBX-FzDa8NI9C3vHeS4Vd4Q?e=Wt8p1I), 2024.

639 Coppola, L., Prieur, L., Taupier-Letage, I., Estournel, C., Testor, P., Lefevre, D., Belamari, S., & Taillandier, V.:
640 Observation of oxygen ventilation into deep waters through targeted deployment of multiple Argo-O₂ floats in the
641 north-western Mediterranean Sea in 2013, *J. Geophys. Res.-Oceans*, 122, 6325–6341,
642 <https://doi.org/10.1002/2016JC012594>, 2017.

643 Coppola, L., Legendre, L., Lefevre, D., Prieur, L., Taillandier, V., & Riquier, E. D. (2018). Seasonal and inter-
644 annual variations of dissolved oxygen in the northwestern Mediterranean Sea (DYFAMED site). *Progress in*
645 *Oceanography*, 162, 187–201, <https://doi.org/10.1016/j.pocean.2018.03.001>, 2018.

Formatted: English (United States)

Formatted: Font: 11 pt, Complex Script Font: 11 pt,
English (United States)

Formatted: English (United States)

Field Code Changed

Formatted: English (United States)

Formatted: English (United States)

Field Code Changed

Field Code Changed

646 Cossarini, G., Feudale, L., Teruzzi, A., Bolzon, G., Coidessa, G., Solidoro, C., Di Biagio, V., Amadio, C., Lazzari,
647 P., Brosich, A., and Salon, S.: High-resolution reanalysis of the Mediterranean Sea biogeochemistry (1999–2019),
648 Front. Mar. Sci., 8, 741486, <https://doi.org/10.3389/fmars.2021.741486>, 2021.

649 Fichaut, M., Garcia, M. J., Giorgetti, A., Iona, A., Kuznetsov, A., Rixen, M., and Medar Group:
650 MEDAR/MEDATLAS 2002: A Mediterranean and Black Sea database for operational oceanography, Elsevier
651 Oceanography Series, 69, 645–648, [https://doi.org/10.1016/S0422-9894\(03\)80107-1](https://doi.org/10.1016/S0422-9894(03)80107-1), 2003.

652 Fourier, M., Coppola, L., Lebrato, M., Testor, P., Bosse, A., D'Ortenzio, F., Taillandier, V., de Madron, X. D.,
653 Mortier, L., Prieur, L., and Gatti, J.: Impact of intermittent convection in the northwestern Mediterranean Sea on
654 oxygen content, nutrients, and the carbonate system, *J. Geophys. Res.-Oceans*, 127, e2022JC018615,
655 <https://doi.org/10.1029/2022JC018615>, 2022.

656 Friedland, R., Macias, D., Cossarini, G., Daewel, U., Estournel, C., Garcia-Gorritz, E., Grizzetti, B., Grégoire, M.,
657 Gustafson, B., Kalaroni, S., Kerimoglu, O., Lazzari, P., Lenhart, H., Lessin, G., Maljutenko, I., Miladinova, S.,
658 Müller-Karulis, B., Neumann, T., Parn, O., Pätsch, J., Piroddi, C., Raudsepp, U., Schrum, C., Stegert, C., Stips,
659 A., Tsiaras, K., Ulses, C., and Vandenbulcke, L.: Effects of nutrient management scenarios on marine
660 eutrophication indicators: a pan-European, multi-model assessment in support of the Marine Strategy Framework
661 Directive, Front. Mar. Sci., 8, 596126, <https://doi.org/10.3389/fmars.2021.596126>, 2021.

662 Garcia and Gordon (1992) "Oxygen solubility in seawater: Better fitting equations", *Limnology & Oceanography*,
663 vol 37(6), p1307-1312.

664 Grasshoff, K., Ehrhardt, M., and Kremling, K.: *Methods of Seawater Analysis*, 2nd Edition, Verlag Chemie
665 Weinheim, New York, 419 p., 1983.

666 Grasshoff, K., Kremling, K., and Ehrhardt, M.: *Methods of seawater analysis* (3rd edn.), Weinheim Press, WILEY-
667 VCH, 203–273, 1999.

668 Grégoire, M., Oschlies, A., Canfield, D., Castro, C., Ciglenečki, I., Croot, P., Salin, K., Schneider, B., Serret, P.,
669 Slomp, C.P., Tesi, T., Yücel, M. (2023). Ocean Oxygen: the role of the Ocean in the oxygen we breathe and the
670 threat of deoxygenation. Rodriguez Perez, A., Kellett, P., Alexander, B., Muñiz Piniella, Á., Van Elslander, J.,
671 Heymans, J. J., [Eds.] Future Science Brief No. 10 of the European Marine Board, Ostend, Belgium. ISSN: 2593-
672 5232. ISBN: 9789464206180. DOI: 10.5281/zenodo.7941157, 2023.

673 Guy, S.-V., Kress, N., Silverman, J., Gertner, Y., Ozer, T., Biton, E., Lazar, A., Gertman, I., Rahav, E., and Herut,
674 B.: Post-eastern Mediterranean Transient Oxygen Decline in the Deep Waters of the Southeast Mediterranean Sea
675 Supports Weakening of Ventilation Rates, Front. Mar. Sci., 7, <https://doi.org/10.3389/FMARS.2020.598686>,
676 2021.

677 Hainbucher, D., Rubino, A., Cardin, V., Tanhua, T., Schroeder, K., and Bensi, M.: Hydrographic situation during
678 cruise M84/3 and P414 (spring 2011) in the Mediterranean Sea, *Ocean Sci.*, 10, 669-682,
679 <https://doi.org/10.5194/os-10-669-2014>, 2014.

680 Helen, R., Powley, Krom, M. D., Van Cappellen, P.: Circulation and oxygen cycling in the Mediterranean Sea:
681 Sensitivity to future climate change, *J. Geophys. Res.*, <https://doi.org/10.1002/2016JC012224>, 2016.

682 Hoppema, M., Velo, A., van Heuven, S., Tanhua, T., Key, R. M., Lin, X., Bakker, D. C. E., Perez, F. F., Ríos, A.
683 F., Lo Monaco, C., Sabine, C. L., Álvarez, M., and Bellerby, R. G. J.: Consistency of cruise data of the CARINA
684 database in the Atlantic sector of the Southern Ocean, *Earth Syst. Sci. Data*, 1, 63–75, [https://doi.org/10.5194/essd-](https://doi.org/10.5194/essd-1-63-2009)
685 [1-63-2009](https://doi.org/10.5194/essd-1-63-2009), 2009.

686 Janzen, C., Murphy, D., and Larson, N.: Getting more mileage out of dissolved oxygen sensors in long-term
687 moored applications, *OCEANS 2007, IEEE*, doi: 10.1109/OCEANS.2007.4449398, 2007.

688 Johnson, G. C., Robbins, P. E., and Hufford, G. E.: Systematic adjustments of hydrographic sections for internal
689 consistency, *J. Atmos. Ocean. Tech.*, 18, 1234–1244, [https://doi.org/10.1175/1520-](https://doi.org/10.1175/1520-0426(2001)018<1234:SAOHSF>2.0.CO;2)
690 [0426\(2001\)018<1234:SAOHSF>2.0.CO;2](https://doi.org/10.1175/1520-0426(2001)018<1234:SAOHSF>2.0.CO;2), 2001.

Field Code Changed

Field Code Changed

Field Code Changed

Field Code Changed

Field Code Changed

Field Code Changed

Field Code Changed

691 Jullion, L.: TAIPro2016: A Tyrrhenian Sea & Alger-Provençal component of the MedSHIP Programme, RV
692 Angeles Alvarino, 18/08/16 – 29/08/16, Palermo (Italy) – Barcelona (Spain), Bremerhaven, EUROFLEETS2
693 Cruise Summary Report, <https://epic.awi.de/id/eprint/49725/>, 2016.

694 Keeling, R. F., Körtzinger, A., and Gruber, N.: Ocean deoxygenation in a warming world, *Annu. Rev. Mar. Sci.*,
695 2, 199–229, doi: 10.1146/annurev.marine.010908.163855, 2010.

696 Key, R.M., Tanhua, T., Olsen, A., Hoppema, M., Jutterström, S., Schirnack, C., Van Heuven, S., Kozyr, A., Lin,
697 X., Velo, A., Wallace, D.W.R., Mintrop, L., 2010. The CARINA data synthesis project: introduction and overview.
698 *Earth Syst. Sci. Data*, 2, 105–121, <https://doi.org/10.5194/essd-2-105-2010>, 2010.

699 Key, R.M., Kozyr, A., Sabine, C.L., Lee, K., Wanninkhof, R., Bullister, J.L., Feely, R.A., Millero, F.J., Mordy,
700 C., and Peng, T.-H.: A global ocean carbon climatology: Results from Global Data Analysis Project (GLODAP).
701 *Global Biogeochem. Cycles*, 18, GB4031, <https://doi.org/10.1029/2004GB002247>, 2004.

702 Langdon, C.: Determination of Dissolved Oxygen in Seawater by Winkler Titration using Amperometric
703 Technique, In: Hood, E.M., Sabine, C.L., Sloyan, B.M. (Eds.), *The GO-SHIP Repeat Hydrography Manual: A*
704 *Collection of Expert Reports and Guidelines, Version 1*, IOCCP Report Number 14, ICPO Publication Series
705 Number 134, 18pp., <https://doi.org/10.25607/OBP-1350>, 2010.

706 Lauvset, S. K., and Tanhua, T.: A toolbox for secondary quality control on ocean chemistry and hydrographic data,
707 *Limnol. Oceanogr. Methods*, 13, 601–608, <https://doi.org/10.1002/lom3.10050>, 2015.

708 Lauvset, S. K., Lange, N., Tanhua, T., Bittig, H. C., Olsen, A., Kozyr, A., Álvarez, M., Azetsu-Scott, K., Brown,
709 P. J., Carter, B. R., Cotrim da Cunha, L., Hoppema, M., Humphreys, M. P., Ishii, M., Jeansson, E., Murata, A.,
710 Müller, J. D., Pérez, F. F., Schirnack, C., Steinfeldt, R., Suzuki, T., Ulfssbo, A., Velo, A., Woosley, R. J., and Key,
711 R. M.: The annual update GLODAPv2.2023: the global interior ocean biogeochemical data product, *Earth Syst.*
712 *Sci. Data*, 16, 2047–2072, <https://doi.org/10.5194/essd-16-2047-2024>, 2024.

713 Li P and Tanhua T (2020) Recent Changes in Deep Ventilation of the Mediterranean Sea; Evidence From Long-
714 Term Transient Tracer Observations. *Front. Mar. Sci.* 7:594. doi: 10.3389/fmars.2020.00594

715 Liu G., Yu,X., Zhang,J., Wang,X., Xu,N., Ali,S.: Reconstruction of the three-dimensional dissolved oxygen and
716 its spatio-temporal variations in the Mediterranean Sea using machine learning, *Journal of Environmental*
717 *Sciences*,2025,ISSN 1001-0742,<https://doi.org/10.1016/j.jes.2025.01.010>.

718 López-Jurado, J. L., Balbín, R., Alemany, F., Amengual, B., Aparicio-González, A., Fernández de Puellas, M. L.,
719 García-Martínez, M. C., Gazá, M., Jansá, J., Morillas-Kieffer, A., Moyá, F., Santiago, R., Serra, M., and Vargas-
720 Yáñez, M.: The RADMED monitoring programme as a tool for MSFD implementation: towards an ecosystem-
721 based approach, *Ocean Sci.*, 11, 897–908, <https://doi.org/10.5194/os-11-897-2015>, 2015.

722 Manca, B., Burca, M., Giorgetti, A., Coatanoan, C., Garcia, M. J., and Iona, A. Physical and biochemical averaged
723 vertical profiles in the Mediterranean regions: an important tool to trace the climatology of water masses and to
724 validate incoming data from operational oceanography, *J. Mar. Syst.*, 48, 83–116,
725 <https://doi.org/10.1016/j.jmarsys.2003.11.025>, 2004.

726 Macías, D., Garcia-Gorriaz, E., and Stips, A.: Deep winter convection and phytoplankton dynamics in the NW
727 Mediterranean Sea under present climate and future (horizon 2030) scenarios, *Sci. Rep.*, 8, 6626,
728 <https://doi.org/10.1038/s41598-018-24978-5>, 2018.

729 Margirier, F., Testor, P., Heslop, E., Mallil, K., Bosse, A., Houpert, L., Mortier, L., Bouin, M.-N., Coppola, L.,
730 D’Ortenzio, F., Durrieu de Madron, X., Murre, B., Prieur, L., Raimbault, P., and Taillandier, V.: Abrupt warming
731 and salinification of intermediate waters interplays with decline of deep convection in the Northwestern
732 Mediterranean Sea, *Sci. Rep.*, 10, 20923, <https://doi.org/10.1038/s41598-020-77961-9>, 2020.

733 Martínez, J., Leonelli, F. E., García-Ladona, E., Garrabou, J., Kersting, D. K., Bensoussan, N., and Pisano, A.:
734 Evolution of marine heatwaves in warming seas: the Mediterranean Sea case study, *Front. Mar. Sci.*, 10, 1193164,
735 <https://doi.org/10.3389/fmars.2023.1193164>, 2023.

Field Code Changed

Formatted: Font: (Default) +Headings CS (Times New Roman), 10 pt, Font color: Text 1, Complex Script Font: +Headings CS (Times New Roman), 10 pt

Formatted: Font: (Default) +Headings CS (Times New Roman), 10 pt, Font color: Text 1, Complex Script Font: +Headings CS (Times New Roman), 10 pt, English (United States), Pattern: Clear

Formatted: Normal

Formatted: Font color: Auto

Field Code Changed

Formatted: Normal

Formatted: Font color: Auto

Field Code Changed

Field Code Changed

Field Code Changed

736 Marullo, S., De Toma, V., di Sarra, A., Iacono, R., Landolfi, A., Leonelli, F., Napolitano, E., Meloni, D., Organelli,
737 E., Pisano, A., Santoleri, R., and Sferlazzo, D.: Has the frequency of Mediterranean Marine Heatwaves really
738 increased in the last decades? , EGU General Assembly 2023, Vienna, Austria, 23–28 Apr 2023, EGU23-4429,
739 <https://doi.org/10.5194/egusphere-egu23-4429> , 2023.

740 Mavropoulou, A.-M., Vervatis, V., and Sofianos, S.: Dissolved oxygen variability in the Mediterranean Sea, J.
741 Mar. Syst., 208, 103348, <https://doi.org/10.1016/j.jmarsys.2020.103348> , 2020.

742 Mavropoulou, A.-M.: Mediterranean Sea: Dissolved Oxygen, Temperature and Salinity Annual Variability and
743 Monthly Climatology for the period 1960-2011, <https://doi.org/10.5281/zenodo.3878076> , 2020.

744 Middleton, L., Wu, W., Johnston, T. M. S., Tarry, D. R., Farrar, J. T., Poulain, P.-M., Özgökmen, T. M.,
745 Shcherbina, A. Y., Pascual, A., McNeill, C. L., Belgacem, M., Berta, M., Abbott, K., Worden, A. Z., Wittmers,
746 F., Kinsella, A., Centurioni, L. R., Hormann, V., Cutolo, E., Tintoré, J., Ruiz, S., Casas, B., Cheslack, H.,
747 CALYPSO Collaboration, D'Asaro, E. A., and Mahadevan, A.: Ocean cyclone splitting ventilates the upper ocean,
748 Sci. Adv., accepted, 2025.

749 Moriarty, J. M., Harris, C. K., Fennel, K., Friedrichs, M. A. M., Xu, K., and Rabouille, C.: The roles of
750 resuspension, diffusion and biogeochemical processes on oxygen dynamics offshore of the Rhône River, France:
751 a numerical modeling study, Biogeosciences, 14, 1919–1946, <https://doi.org/10.5194/bg-14-1919-2017> , 2017.

752 Olsen, A., Key, R. M., van Heuven, S., Lauvset, S. K., Velo, A., Lin, X., Schirnack, C., Kozyr, A., Tanhua, T.,
753 Hoppema, M., Jutterström, S., Steinfeldt, R., Jeansson, E., Ishii, M., Pérez, F. F., and Suzuki, T.: The Global Ocean
754 Data Analysis Project version 2 (GLODAPv2) – an internally consistent data product for the world ocean, Earth
755 Syst. Sci. Data, 8, 297–323, <https://doi.org/10.5194/essd-8-297-2016> , 2016.

756 Olsen, A., Lange, N., Key, R. M., Tanhua, T., Bittig, H. C., Kozyr, A., Álvarez, M., Azetsu-Scott, K., Becker, S.,
757 Brown, P. J., Carter, B. R., Cotrim da Cunha, L., Feely, R. A., van Heuven, S., Hoppema, M., Ishii, M., Jeansson,
758 E., Jutterström, S., Landa, C. S., Lauvset, S. K., Michaelis, P., Murata, A., Pérez, F. F., Pfeil, B., Schirnack, C.,
759 Steinfeldt, R., Suzuki, T., Tilbrook, B., Velo, A., Wanninkhof, R., and Woosley, R. J.: An updated version of the
760 global interior ocean biogeochemical data product, GLODAPv2.2020, Earth Syst. Sci. Data, 12, 3653–3678,
761 <https://doi.org/10.5194/essd-12-3653-2020> , 2020.

762 Olsen, A., Key, R. M., van Heuven, S., Lauvset, S. K., Velo, A., Lin, X., Schirnack, C., Kozyr, A., Tanhua, T.,
763 Hoppema, M., Jutterström, S., Steinfeldt, R., Jeansson, E., Ishii, M., Pérez, F. F., and Suzuki, T.: The Global Ocean
764 Data Analysis Project version 2 (GLODAPv2) – an internally consistent data product for the world ocean, Earth
765 Syst. Sci. Data, 8, 297–323, <https://doi.org/10.5194/essd-8-297-2016> , 2016.

766 Olsen, A., Lange, N., Key, R. M., Tanhua, T., Álvarez, M., Becker, S., Bittig, H. C., Carter, B. R., Cotrim da
767 Cunha, L., Feely, R. A., van Heuven, S., Hoppema, M., Ishii, M., Jeansson, E., Jones, S. D., Jutterström, S.,
768 Karlsen, M. K., Kozyr, A., Lauvset, S. K., Lo Monaco, C., Murata, A., Pérez, F. F., Pfeil, B., Schirnack, C.,
769 Steinfeldt, R., Suzuki, T., Telszewski, M., Tilbrook, B., Velo, A., and Wanninkhof, R.: GLODAPv2.2019 – an
770 update of GLODAPv2, Earth Syst. Sci. Data, 11, 1437–1461, <https://doi.org/10.5194/essd-11-1437-2019> , 2019.

771 Owens, W. B., and R. C. Millard Jr., 1985: A new algorithm for CTD oxygen calibration. J. Physical
772 Oceanography., 15, 621–631.

773 Pastor, F., and Khodayar, S.: Marine heat waves: Characterizing a major climate impact in the Mediterranean,
774 EGU General Assembly 2023, Vienna, Austria, 24–28 Apr 2023, EGU23-13058,
775 <https://doi.org/10.5194/egusphere-egu23-13058> , 2023.

776 Reale, M., Cossarini, G., Lazzari, P., Lovato, T., Bolzon, G., Masina, S., Solidoro, C., and Salon, S.: Acidification,
777 deoxygenation, and nutrient and biomass declines in a warming Mediterranean Sea, Biogeosciences, 19, 4035–
778 4065, <https://doi.org/10.5194/bg-19-4035-2022> , 2022.

779 Ribotti, A., Sorgente, R., Pessini, F., Cucco, A., Quattrocchi, G., and Borghini, M.: Twenty-one years of
780 hydrological data acquisition in the Mediterranean Sea: quality, availability, and research, Earth Syst. Sci. Data,
781 14, 4187–4199, <https://doi.org/10.5194/essd-14-4187-2022> , 2022.

Field Code Changed

Field Code Changed

Field Code Changed

Field Code Changed

Field Code Changed

Formatted: Space Before: 0 pt, Line spacing: Multiple
1,08 li

Formatted: Font: Font color: Auto, English (United
States)

Field Code Changed

Field Code Changed

Field Code Changed

827 Ulses, C., D'Ortenzio, F., Coppola, L., Estournel, C., Testor, P., Marsaleix, P., Prieur, L., Taillandier, V., Dumas,
828 F., Severin, T., and Conan, P.: Oxygen budget of the north-western Mediterranean deep-convection region,
829 *Biogeosciences*, 18, 937–960, <https://doi.org/10.5194/bg-18-937-2021>, 2021.

830 Yao, M., Marcou, O., Goyet, C., Guglielmi, V., Touratier, F., and Savy, J.-P.: Time variability of the north-western
831 Mediterranean Sea pH over 1995–2011, *Mar. Environ. Res.*, 116, 51–60,
832 <https://doi.org/10.1016/j.marenvres.2016.02.016>, 2016.

Field Code Changed